The Application of the Electron Microscope, the Optical Microscope, and the Electron Diffraction Camera to the Study of Fine Structure.

By

M.M.Bluhm.

A Thesis Submitted for the

Diploma of the Imperial College.

Applied Physical Chemistry
Laboratories,

Imperial College.

June, 1951.

Abstract of Thesis

Entitled

The Application of the Electron Microscope, the Optical Microscope, and the Electron Diffraction Camera to the Study of Fine Structure.

by

M.M. BLUHM.

The limitation of the resolving power of the optical microscope is discussed, and an account is given of the operation and construction of a phase contrast microscope, which was found to be a valuable adjunct to the electron microscope.

The electron microscope constructed in this laboratory and modified by the writer is described in outline, and the factors limiting its resolving power are discussed in detail. The formation of electron optical images with and without a limiting aperture in the objective lens is considered for objects differing in mass thickness. The effect of increasing the high tension voltage is discussed.

The above optical and electron microscopes were applied to the study of the polished layer on glass surfaces, and Beilby's views on the flow of the polish layer were confirmed.

Myofibrils from rat diaphragm were examined by phase contrast microscopy to observe the changes occurring in the preparation of the material for examination by the electron microscope. Myofibrils were then examined by electron microscopy, and certain changes in length and structure were observed in different states of activity produced by passive stretching and stimulation.

Finally, silver films evaporated in vacuo at different temperatures on to rocksalt cleavage faces were studied by means of electron microscopy and by electron diffraction, but the electron micrographs added little to the knowledge previously obtained by the, in this case, far more informative technique of electron diffraction.

CONTENTS.

Page

GENERAL INTRODUCTION.

A knowledge of the arrangement in space of atoms, molecules and groups of molecules is an essential step in our search for a better understanding of the physical world. The simple microscope was the first instrument used to extend the range of the human eye. Two convex lenses were soon combined to form the more powerful compound microscope, and important new advances in biology and physics followed whenever a better method was found for correcting the aberrations of object glasses. A limit to this process appeared to have been reached when lens systems could be designed and made with such a degree of perfection that the wavelength of light alone imposed a lower limit, in the region of 2400 A., on the size of objects and their structure that could be resolved. Only comparatively minor advances resulted from the use of ultra-violet light as a means of increasing the resolving power.

A new impetus to the study of fine structure of surfaces and thin films or objects was given by the experimental demonstration of the wave nature of the electron, and within a short space of time electron diffraction and electron microscopy had in many directions superseded optical microscopy. The electron microscope, as its name implies, can be regarded as a development of the

optical microscope, using electron waves instead of light waves to form an image of the object. The resolving power of the electron microscope is better by about two orders than that of its optical counterpart, and is not yet limited by the wavelength of the moving electron, but rather by considerations of lens design and supply stability.

Owing to the electronic charge, the cathode rays penetrate, at all events elastically, only a small thickness of matter in the solid or liquid state. Consequently, objects examined in the electron microscope must be extremely thin, and therefore have often to be isolated from their normal natural environment. This greatly increases the difficulties in specimen preparation, and in the interpretation of the electron micrograph.

The information afforded by electron diffraction is complementary to that obtained by electron microscopy. The diffraction pattern reflects the average arrangement in space of the atoms and molecules of that part of the object which is flooded by the electron beam. The greater the orderliness of this arrangement, the fuller and more detailed is the information. Electron diffraction has been applied extensively to the study of fine structure of thin films and surfaces. Under suitable conditions, the crystal

structure, orientation, habit and size, the surface smoothness on an atomic scale, and atomic and molecular spacings of only a few angstroms can be deduced from the diffraction pattern.

Multiple beam interferometry can be used to detect differences in niveau of the order of atomic dimensions, provided that they are of sufficient extent to be resolved by a high power objective.

No attempt will be made to review the work done with each of the instruments considered. Although all these techniques are now well established, their complexity is such that they are only rarely employed together. The present work is an attempt to explore this possibility, bearing in mind the type of information required in each problem, since in many cases one instrument alone will supply the desired answer. It was found that the optical microscope was almost invariably required as an aid to the electron microscope, and that the combined use of the techniques of electron microscopy and electron diffraction holds out the greatest hope of progress for the future.

I. THE CONSTRUCTION AND PERFORMANCE OF THE INSTRUMENTS.

1. Introduction.

The diffraction pattern, and consequently also the image, bears a unique relation to the specimen. This relation depends on the nature of the radiation and on the properties of the instrument. The value of the information obtained from the patterns or images depends in each case on our knowledge of this relation.

The optical and electron microscopes, as well as the electron diffraction camera, are all complex instruments, in that their design represents a compromise between conflicting requirements. For present purposes, the normal optical microscope need only be considered briefly, though the important recent developments in the use of phase contrast microscopy will have to be discussed in some detail. The phase contrast microscope, using transmitted or incident light, is particularly useful as an aid to the electron microscope, since their images are by nature remarkably similar in appearance and significance, although their contrast and image formation are based on entirely different principles.

The three-stage electron microscope with electromagnetic lenses will be discussed in some detail. It can be used as a microscope as well as a diffraction camera for

transmission patterns, and it is still in a comparatively early stage of development. Certain modifications to the instrument in this laboratory will be suggested.

The electron diffraction camera is simple in operation, and the interpretation of diffraction patterns has been put on a mathematical basis, which is now so firmly established that only the methods required in the present work need be described.

2. THE OPTICAL MICROSCOPE.

(i) Description of the Apparatus.

A conventional microscope stand (Beck, London, Model 29) was used for the examination of transparent specimens, and a similar model (Beck, London, Laboratory Metallurgical Microscope with Wrighton-Beck Illuminator) for opaque specimens. A Beck eyepiece camera (No. 3654) with a fixed camera length of 18 cm. served for taking photomicrographs, and an "Osira" mercury vapour lamp (G.E.C. Wembley) was used as a source after removing its glass envelope, except for vertical illumination, when a tungsten filament lamp with an illuminating system clamped to the body tube of the microscope was found to be more convenient. Some relevant data of the optical systems normally employed in this work are shown in Table I.

TABLE I.

Achromatic Objective				Huyghensian Eyepiece	Magnification at	
Focal Length	N.A.	Resolving Power $\lambda = 5460$	Depth of Focus		18 cm.	25 cm.
16 mm.	0.28	12000A.	0.008 mm.	x 10	x 75	x 100
4 mm.	0.85	3900A.	0.0007 mm.	x 10	x 315	x 440

The figures for the magnification at 25 cm. (the value

normally taken for the least distance of distinct vision) were calculated from those at 18 cm., which were obtained by direct measurment.

A well-corrected lens was used as the effective source, and an iris diaphragm placed near it controlled the size of the illuminated area of the object. The iris diaphragm of the Abbe condenser (1.0 N.A.) controlled what proportion of the aperture of the objective was filled with direct light. The wavelength of the illumination was generally restricted to a narrow band in the green part of the spectrum (Chance-Parson Filter No. 3), and its intensity could be reduced with a neutral filter (Chance-Parson Filter No. 10). In this way, critical illumination could be secured for objectives up to about 1.0 N.A.

A few micrographs were taken with the Vickers Projection Microscope, which is fully described in the descriptive booklet published by the manufacturers (Messrs. Cooke, Troughton & Simms, Ltd.).

(ii) Resolving Power and Critical Illumination. The Rayleigh Limit.- We owe to Rayleigh (1896, see also Helmholtz, 1874) an elegant discussion of resolving power applicable to all optical instruments. Rayleigh showed that the smallest distance ε between two self-luminous

points that can be imaged separately by an aplanatic system, is given by

$$\varepsilon = \frac{1}{2} \frac{\lambda}{\mu \sin\alpha}$$

where λ is the wavelength in vacuo, μ the refractive index of the object space, and α the semi-angular aperture of the system. The value of the numerical factor depends on the minimum distance between the two images which is regarded as constituting separation. It is now customary to take

$$\varepsilon = \frac{0.61\,\lambda}{N.A.}$$

where N.A. $= \mu \sin\alpha$ is the numerical aperture. This factor is based on a separation of the images by the radius of the Airy disc formed by diffraction at a circular aperture (Airy, 1835). It is therefore evident that the wave nature of light prevents optical instruments from forming geometrically exact images.

Johnson (1928) has shown experimentally that modern microscope objectives are capable of almost the resolving power given by this formula, in other words, they behave very nearly like an aplanatic system, even at the high numerical apertures (up to 1.4 N.A.) used in optical microscopy.

Critical Illumination.- It must, however, be admitted that the normal microscope object is far from being a self-luminous point. Rayleigh (1896) gave convincing, though not

mathematically precise, reasons for the view that a condenser system of an optical excellence and a numerical aperture equal to that of the objective illuminates any thin object in such a way that no phase relation exists between light from different areas of the object of the size resolved by the objective. This realisation is the basis for the insistence on the use of critical illumination, and can be obtained in practice by the use of a well-corrected condenser system of almost the same numerical aperture as the objective. Critical illumination has been used by practical microscopists for over 50 years, and a detailed theoretical discussion of the behaviour of different objects met with in practice need not concern us here (see Martin, 1932).

The Abbe Theory.- Another theory of microscopic vision, originally due to Abbe (1873), was discussed in detail by Conrady (1904, 1905), and put into final form by Lummer and Reiche (1910). The Abbe Theory is mentioned here not so much for its considerable historical interest, but because it forms a convenient basis for an elementary discussion of phase contrast. The object is regarded as an amplitude grating O illuminated by parallel light. (fig. 1.). The aplanatic lens system L (the objective) forms an enlarged image O_i' of each object O_i. The grating diffracts light in the well-known manner, and diffraction

images of the source are formed at S_0, S_1, ... near the back focal plane of the lens system L'. These diffraction images may, in turn, be regarded as secondary sources, and give rise to interference bands. The theory states that the cooperation of all the secondary sources is required to image an object O_1 at O_1' in the image plane. If at least one first order spectrum can enter the objective, the grating is just resolved, and it can be shown that the value obtained for ε is the same as that obtained by Rayleigh's method. As the number of spectra able to enter the objective is increased, the image more and more nearly corresponds to the object.

Some very beautiful experiments illustrating this theory were described by Rayleigh (1896), who also pointed out some of its limitations. Martin (1931), in a more rigorous treatment, showed that both Abbe's and Rayleigh's point of view appeared in the analysis, and discussed some of the diffraction effects obtained from simple objects at a distance of less than ε apart. Rayleigh's and Abbe's treatments must therefore be regarded as alternative physical models of the mechanism of microscopic vision, and both are found to lead to the same results.

Vertical Illumination.- Opaque specimens are generally examined in an optical microscope fitted with one of the well-known forms of vertical illuminator (Martin and Johnson, 1949). In this arrangement, the condenser is re-

placed by the objective, which thus fulfils a dual purpose. In principle, the same theory of microscopic vision holds, as for transmitted light, and critical illumination can be obtained. The practical difficulties arising out of this arrangement can be largely overcome, and need not be discussed here.

(iii) The Phase Contrast Microscope.

Other Methods of Obtaining Contrast.- With critical illumination and transmitted light, contrast between different parts of the object is in general the result of differences in their absorption of light. This is satisfactory for many types of specimen, and contrast can be enhanced by the use of stains. For certain types of specimen, ultra-violet light gives better contrast, and for materials exhibiting birefringence, polarized light has long been used to the same end. A number of other methods for enhancing contrast (oblique and dark ground illumination, illumination by a narrow pencil) have been practiced for a long time, but although they are useful for some purposes, the resulting images are difficult or even uncertain in interpretation. The most promising recent development towards increasing contrast has been the application of the phase contrast principle to optical microscopy by Zernike in 1932.

With critical illumination at normal incidence,

contrast between different parts of the object is due either to differences in reflectivity, or to comparatively sharp steps in the surface which reflect light away from the objective. The remarks with regard to contrast made in connection with illumination by transmitted light apply in this case, except that etching takes the place of staining. The phase contrast principle was applied to metal specimens by Cuckow (1949), who realised its special value as "a pilot instrument in electron metallography".

The Development of the Phase Contrast Microscope.- The principle of phase contrast as applied to the optical microscope was enunciated by Zernike in 1932, and the literature has grown rapidly in the last few years. For a review of the principles of the subject, the construction of phase plates and other technical details, and a good bibliography, Brice (1947) may be consulted, and only a few important references will be mentioned here.

An elementary vector treatment based on Abbe's Theory was given by Zernike (1935), and a rigorous mathematical treatment is due to the same author (1942). Koehler and Loos (1941) published a fuller version of the graphical vector treatment, and Burch and Stock (1942) described the construction of a simple phase plate for obtaining phase contrast with a slit source. The use of polarised

light for obtaining phase contrast of variable amplitude and phase, originally due to Osterberg (1946), was developed concurrently by Taylor (1947) and Paine (1950) in this country. An extensive practical study of the possibilities of this apparatus was made by Oettle (1950). Finally, phase contrast for opaque specimens was described by Cuckow (1949).

An Explanation of Phase Contrast.- Following Zernike (1935), an amplitude and a phase grating*are compared in order to explain the operation of the phase principle. Both gratings are illuminated by parallel light, and form diffraction images of the source near the back focal plane of the objective (Abbe's Theory, fig. 1). As will be shown later, these diffraction images may be similar in intensity (depending on the degree of absorption and phase shift introduced by the gratings), but they must differ in phase, since the images of the objects which they produce in the final image plane I are entirely different; the image of the amplitude grating shows alterations in intensity, whereas the image of the phase grating shows only variations in phase, which cannot, of course, be detected by the eye or the photographic plate.

---

*An amplitude grating is a regular structure made up of alternate bars, which permit light to pass through them with or without absorption. The bars do not affect the phase of the light. A phase grating is a similar structure, but the alternate bars permit light to pass through them with or without phase shift. These bars do not absorb light.

The vector diagrams (fig.2) represent the wavelets leaving the two types of grating in amplitude and phase. $\overrightarrow{OP}$ and $\overrightarrow{OP'}$ (fig. 2a) are the vectors representing the two kinds of wavelets leaving the amplitude grating, and $\overrightarrow{OP}$ and $\overrightarrow{OP''}$ those leaving the phase grating. The vector $\overrightarrow{OP'}$ in fig. 2a can be decomposed to give the vectors shown in fig. 3a, where $\overrightarrow{OA}$ is defined by

$$\overrightarrow{OP'} = \overrightarrow{OP} + \overrightarrow{OA} ,$$

and, similarly, $\overrightarrow{OP''}$ in fig. 2b can be decomposed to give the vectors in fig. 3b, where $\overrightarrow{OP_h}$ is defined by

$$\overrightarrow{OP''} = \overrightarrow{OP} + \overrightarrow{OP_h} .$$

It will be seen that the vector $\overrightarrow{OP}$ remains the same throughout all portions of both gratings, and represents the background illumination, which is not diffracted. The vector $\overrightarrow{OA}$ represents the light absorbed by the absorbing portions of the amplitude grating, and the vector $\overrightarrow{OP_h}$ represents the light of different phase caused by the phase shifting portions (due to differences in thickness or refractive index) of the phase grating. If the phase shift is small compared with 90° (i.e. the path difference introduced by the phase shifting portions of the grating is small compared with $\frac{\lambda}{4}$), $\overrightarrow{OP_h}$ is nearly perpendicular to $\overrightarrow{OP}$. To this approximation, the zero order spectrum represents only the background illumination, and the higher order spectra r

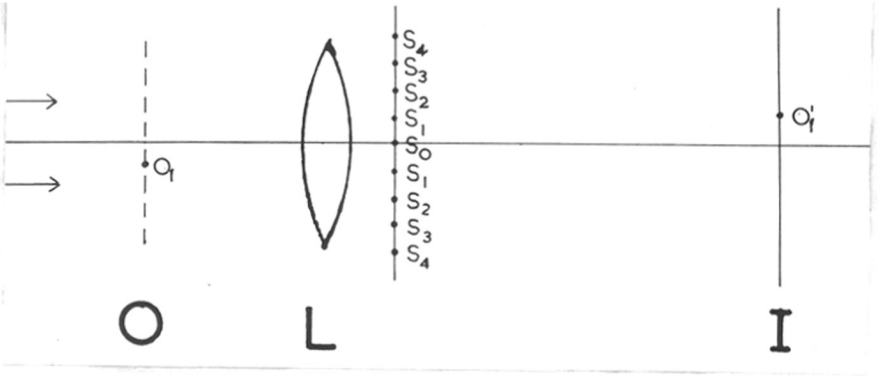

Fig. 1. The formation of images according to the Abbe Theory.

Fig. 2. The vectors representing the wavelets leaving alternate bars of (a) an amplitude and (b) a phase grating.

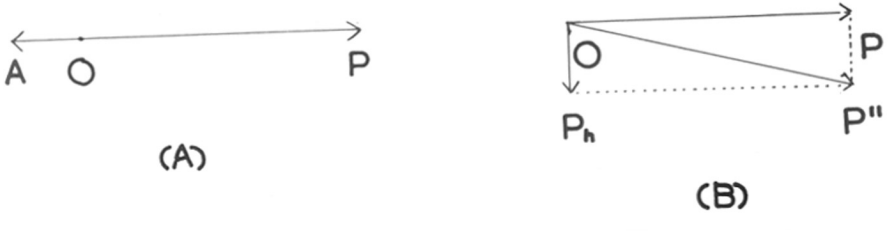

Fig. 3. The vectors shown in fig. 2, each decomposed into two vectors at right angles.

produced by the two gratings differ in phase by 90°. The amplitudes of the higher order spectra merely represent different degrees of absorptivity or phase shift in the object. It follows that a phase grating can be rendered visible by artificially advancing (positive phase contrast) or retarding (negative phase contrast) the phase of the direct image of the source in the back focal plane of the objective by 90°.

The Condition for Maximum Contrast.- To obtain maximum contrast, the illumination must be reduced to zero in some parts of the field. This can only occur by destructive interference between the wavelets represented by the vectors $\overrightarrow{OP}$ and $\overrightarrow{OP}_h$. But for the small phase shifts considered, $\overrightarrow{OP}$ is much greater than $\overrightarrow{OP}_h$. It is therefore necessary to absorb a suitable proportion, depending on the phase shift introduced by the phase grating, of the zero order spectrum, i.e. to reduce the amplitude of the vector $\overrightarrow{OP}$, in order to obtain the maximum phase contrast effect.

The Experimental Arrangements.- The artificial phase shift of 90° and the partial absorption of the zero order spectrum are best carried out by employing an annular source (obtained by inserting an annular aperture in the first focal plane of the condenser), and a combined phase shifting and absorbing annulus in the back focal plane of the objective. This

arrangement gives the minimum coincident area between zero and higher order spectra in the back focal plane of the objective, and illuminates the object symmetrically, thus reducing to a minimum any confusing diffraction effects due to the phase ring.

The apparatus used throughout most of this work was constructed along these lines. Phase rings of suitable characteristics were inserted into existing objectives by Messrs. R. & J. Beck, Ltd., The writer prepared in this laboratory annular diaphragms for each objective, of such dimensions as to give a direct image coincident with the phase ring when placed on the optical axis in the first focal plane of an Abbe condenser. Provision for the lateral movements of the annular apertures was made.

Objects examined in practice are never entirely invisible when viewed with amplitude contrast (normal) illumination, but an impression of the degree of improvement that can be expected in suitable cases may be gained from figs. 10 and 12.

As explained above, different phase retardations produced by the object require a different percentage absorption in the phase plate to produce maximum contrast. An instrument with continuously variable absorption as well as phase shift was described by Paine (1950), and was based on the use of polarized light. After exhaustive tests, Oettle

(1950) found that for most microscopical work, the ability to vary the phase was not particularly useful, since the best results were generally obtained with a phase shift of ± 90°. He also found that objectives with phase rings of three different absorptivities (0%, 80%, 95%) should be available to get the best possible results in the examination of objects differing in the phase shift they introduce.

Phase Contrast Illumination with Incident Light.- Cuckow (1949) has described some interesting applications of phase contrast illumination to metallographic specimens. In this context, the phase contrast microscope must be regarded as an instrument for detecting differences in level, and translating them into differences in intensity in the final image, as distinct from the interferometer, which measures these differences in level. Cuckow rightly stressed the importance of comparing images obtained with amplitude and phase contrast, and developed an instrument, utilising polarised light, with a field divided into two parts, one showing amplitude, and the other phase contrast. A similar comparison can, of course, be made by removing the annular aperture (in the first focal plane of the condenser) from the beam of light. Reference may be made to Cuckow's paper for a bibliography of phase contrast illumination with incident light.

3. THE THREE-STAGE ELECTRON MICROSCOPE.

(i) Introductory.

Electrons were at first regarded as small and light negatively charged particles, since this concept gave a satisfactory account of the experimental observations relating to electrolytic and gaseous conduction, as well as to photo-electric and thermionic emission. Although it was apparently unnecessary to modify this view as a result of Lenard's early experiments on the scattering of cathode rays, a more complex concept of the nature of the electron was required to account adequately for the later observations on the interaction of electrons and matter.

In 1924, de Broglie predicted that moving electrons were associated with a train of waves of wavelength λ given by

$$\lambda = \frac{h}{mv} \approx \sqrt{\frac{150}{V}}$$

where h is Planck's constant, and m the mass and v the velocity of the electrons. V is the accelerating potential. After making a small relativity correction, this expression gives a wavelength of about 0.05 A. for electrons accelerated through 50 kV. De Broglie's prediction was confirmed experimentally by Davisson and Germer (1927) and independently by G.P. Thomson and A. Reid (1927).

In the meantime, Busch (1926) discussed the lens properties of axially symmetrical magnetic and electric fields,

and the subsequent construction of uncorrected electron lenses made the electron microscope a practical possibility. A resolving power about 100 times better than that of the light microscope was realised as a result of the extremely short wavelength of the moving electrons, although the continued use of uncorrected lens systems restricted the angular aperture of the objective lens to about 5×10^{-3} radians.

Since the first transmission microscope was constructed by Knoll and Ruska (1932), the literature has grown considerably. An exhaustive bibliography for papers published up till 1948 was edited by Cosslett (1950), and a number of textbooks and monographs dealing with the instrument and the preparation of specimens are now available (von Borries, 1949, Drummond, 1950, Gabor, 1947, Wyckoff, 1949, Zworykin et al., 1945). Only a few relevant papers will, therefore, be cited here.

(ii) Description of the Apparatus.

The instrument in this laboratory has three stages of magnification, and makes use of electro-magnetic lenses. It was constructed by Drs. J.F. Brown (1949) and C.E. Challice (1949) under the direction of Professor G.I. Finch, F.R.S., and has been modified by the writer with a view to increased ease of operation. It is intended to describe it in outline,

and only to discuss in detail those factors which influence its performance.

Description of the Instrument.- The instrument is shown diagrammatically in fig. 4. The electron gun is of conventional design, and consists of a V-shaped tungsten filament surrounded by a self-biassed Wehnelt cylinder to control the electron beam. Insulation between anode and cathode is provided by a glass envelope. The gun was designed to withstand an accelerating voltage of 80 kV., but has occasionally been used up to 120 kV., which at present constitutes the limitation on the operating voltage of the instrument.

There are five electron lenses (computed for an operating voltage of 150 kV.); the condenser, the objective, two alternative intermediate lenses, and the projector lens. Only one of the intermediate lenses is used at a time. The object of this duplication was to simplify the problems of lens design inherent in the computation of a lens capable of a wide variation in focal length without introducing unnecessary aberrations. The specimen, in a suitable holder, is inserted into the mechanical stage, so that it can be moved at right angles to the electron-optical axis within the objective pole pieces. The final image is formed on the fluorescent screen, which can be removed from the path of the electrons to expose a photographic plate. Ilford Half

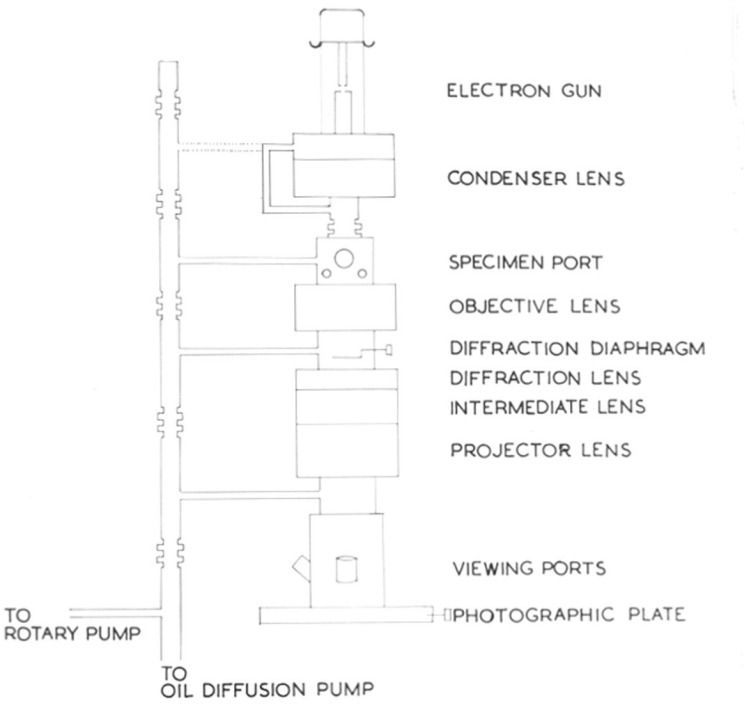

Fig. 4. Diagram of the three-stage electron microscope in this laboratory.

Tone Plates were generally used.

A vacuum of 10^{-4} mm. Hg or better can be obtained in about 10 minutes by means of a Metropolitan-Vickers D.R.1. rotary pump backing an 03B oil diffusion pump.

Electrical Supplies.- The high tension supply was constructed by Messrs. Ferranti Ltd. and is fed from the mains. It consists essentially of a low frequency voltage doubling circuit, and has a maximum output voltage of 200 kV. The output capacity is 0.015 μF., and a saturated diode valve acts as a limiting resistance. The output of this supply is unstabilised and a rough calculation shows that the ripple voltage does not exceed 3 parts in 10^4 of the D.C. voltage (100 kV.) at a current drain of 25 μA. The output voltage does not drift appreciably, provided that there are no abrupt variations in the mains supply.

The current for energising each lens is obtained from separate power packs feeding four electronic stabilising circuits (Challice,1949). Measurement of the ripple voltage by means of a cathode ray oscillograph shows that the ripple current in the objective lens does not exceed 6 parts in 10^6 of the direct current. The circuits are free from drift over periods of a few seconds.

The filament is heated by alternating current supplied by a filament transformer fed from the mains, and the self-

bias of the Wehnelt cylinder introduces a certain amount of stabilisation of the electron beam.

The Ray Path through the Instrument.- The employment of three stages of magnification, apart from shortening the physical length of the instrument and greatly increasing the range of magnification obtainable by varying the lens currents (1500 to 20000 diameters or more), enables diffraction patterns or images of the same part of the specimen to be obtained on the final screen by altering the strength of the intermediate lens. The approximate ray paths through the instrument in the normal high magnification working condition, in the diffraction condition, and in a second image forming condition especially suitable for low magnifications are shown diagrammatically in fig. 5.

(iii) The Formation of Images.

Absorption of Electrons.- The thin objects generally studied by electron microscopy absorb only a negligible proportion of the beam electrons (between 1 in 100 and 1 in 1000), and different proportions of the specimen can have only slight differences in absorptivity. Contrast is therefore not primarily the result of absorption, as it is in the light microscope (except with certain forms of illumination, such as phase contrast), but will be shown to be a consequence of the scattering of electrons by matter.

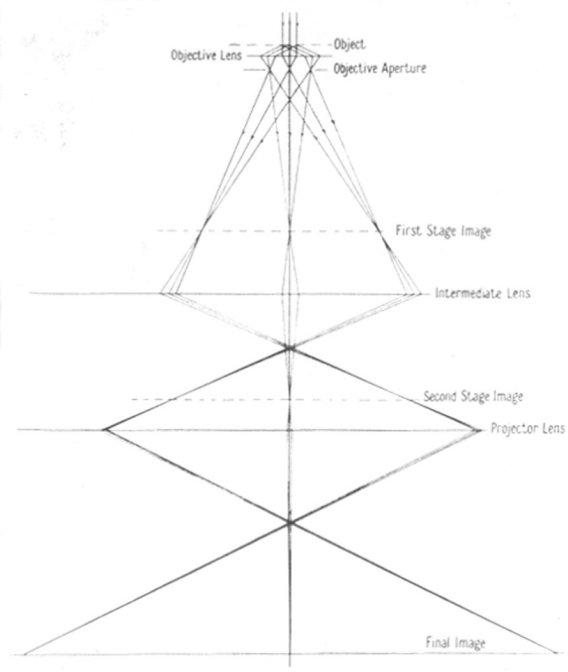

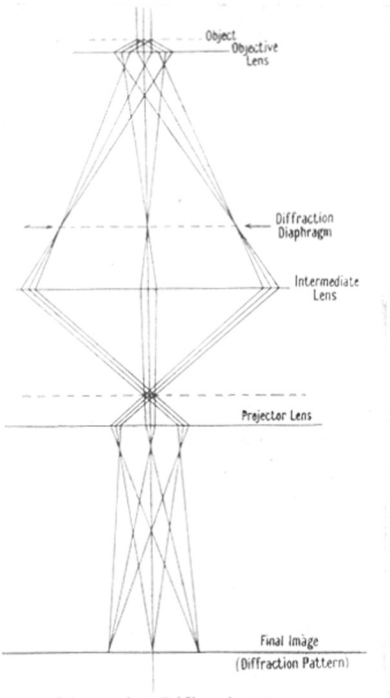

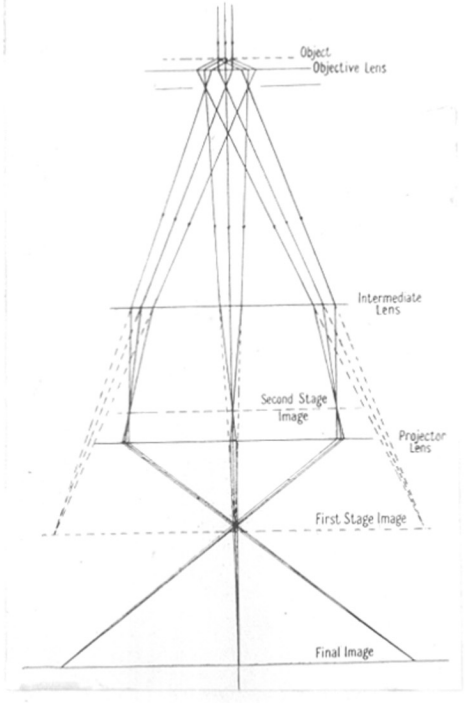

Fig. 5. The ray paths through a three-stage electron microscope in

(a) the normal high magnification working condition

(b) the diffraction condition

(c) the image forming condition especially suitable for low magnifications.

(Reproduced from Proc. Phys. Soc. B, Vol. 63, p. 59, 1950.)

Scattering of Electrons.- When a parallel beam of electrons impinges on a thin homogeneous foil, some of the electrons are scattered by the atoms of the foil; the proportion of the electrons scattered depends, inter alia, on the thickness of the foil and on the atomic number of the atoms of which the foil is composed. Each electron may be scattered either several times (multiple scattering), once, or not at all, either with or without loss of kinetic energy (inelastic or elastic scattering). Inelastic scattering results in an increase in the wavelength associated with the moving electron. After passing through a thin foil, a parallel beam of electrons associated with wavelength contains substantially the same number of electrons as before, but the beam will become divergent, and the wavelength λ associated with the moving electrons will vary between λ and $\lambda + \Delta\lambda$.

Elementary beams.- In the absence of any scattering material in the object plane, the electron intensity in the image plane of the objective, and hence of the projector, is arranged to be practically uniform. If the incident beam is parallel, the resultant intensity in the image plane can be considered as made up of a number of elementary beams, so that each small area in the image plane is illuminated by an elementary beam that has passed

through a corresponding small area in the object plane. If a thin piece of scattering material is introduced into the object plane, the elementary beam corresponding to that area will become divergent, mainly due to elastic scattering, and the distribution of electrons within the beam is shown diagrammatically in fig. 6.

The Effect of an Objective Aperture.- The divergence of the elementary beam can be limited to α_0 by introducing an aperture of suitable size into the objective lens, thus excluding part of the electrons. As a result, the electron intensity in the image plane will be less in the area illuminated by this elementary beam than in the remainder of the image plane. If the value of α_0 is chosen so that the spherical aberration is small, the area of reduced electron intensity can be regarded as an "image" of the piece of scattering material.

Contrast without an Objective Aperture.- It is found in practice that contrast not mainly due to absorption can be obtained without using a small objective aperture. For small values of the divergence of the beam (α), the spherical aberration of each lens is proportional to α^3. As a result, those electrons which have been scattered through large angles (represented by the area under the foot of the curve in fig. 6) suffer greater spherical aberration than those

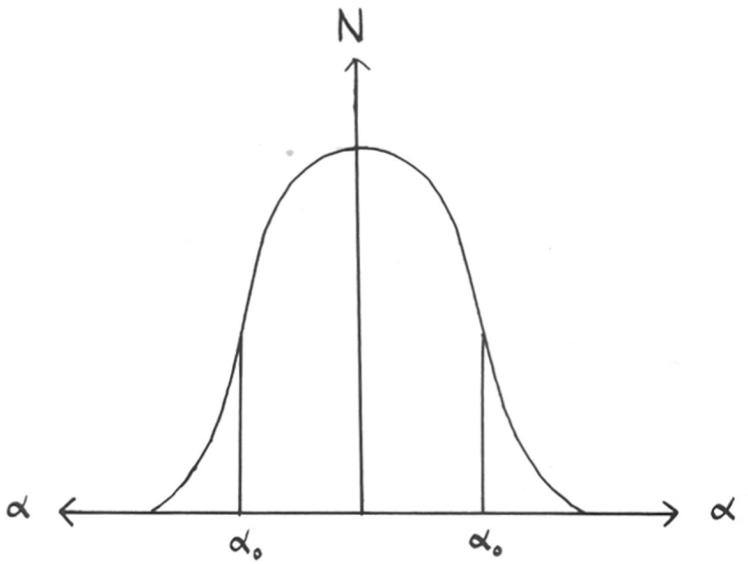

Fig. 6. The distribution of electrons in an elementary beam after scattering by a thin piece of scattering material in the object plane (qualitative).

N = Number of electrons scattered between the angles α and $\alpha+\delta\alpha$.
α = Divergence from the primary beam direction.

scattered through smaller angles. Consequently, a considerable proportion of the electrons in the elementary beam arrive at the final screen outside the area of the "image" (see above), which is therefore again an area of smaller electron intensity than its surroundings. It follows that the appearance of the image formed by the electron microscope depends, inter alia, on the size of the objective aperture.

Chromatic Aberration due to Inelastic Scattering.- Chromatic aberration is proportional to the change in electron velocity. Consider the effect on the contrast of the image if only a small proportion of the electrons in the elementary beam is scattered inelastically, i.e. with a reduction in velocity. Some of the inelastically scattered electrons will arrive outside the area of the "image" (see above), and will contribute to the electron intensity of the surrounding area, in other words, chromatic aberration operating on inelastically scattered electrons may, in some cases, enhance contrast.

Some Final Considerations.- In crystalline objects, Bragg reflections may affect the distribution of electron intensity in the final image. The same is true of certain contour effects (Fresnel fringes, see Hillier, 1940, and phase contrast which can occur at edges and throughout thin objects, see Gabor, 1942-3, 1947), especially if the image is not accurately focussed.

The gradation of electron intensity in the final

image reflects primarily the distribution of mass in the object. It is therefore convenient to define the mass thickness of an object as the product (density x thickness). With certain reservations, the above discussion of image formation shows that an area of high electron intensity in the image corresponds to an area of low mass thickness in the object.

(iv) Resolving Power.

The factors determining the resolving power of the electron microscope will now be considered. They are the wavelength of the moving electron, the aberrations of electron lenses, and the mechanical and electrical design and stability of the instrument and its associated circuits.

Errors due to Diffraction and Spherical Aberration.- An investigation of the properties of electron lenses, such as that given by Cosslett (1946), shows that they suffer from the same kind of aberrations as light optical lenses, but additional aberrations are introduced by the rotational character of the field. Scherzer (1936) has shown theoretically that electron lenses, whether magnetic or electrostatic, must remain uncorrected for spherical aberration in the absence of currents or space charge effects in the path of the electrons. The lenses used in present day electron microscopes are uncorrected, and high magnification images are obtained by using extremely small apertures.

Rayleigh's treatment (1896) of the resolving power of optical systems is applicable to the electron microscope, and shows that, for small values of α, a point source is imaged as a disc* of diameter d_d given by

$$d_d = \frac{\lambda}{\alpha},$$

where λ is the wavelength associated with the moving electrons, and α the divergence of the beam entering the objective lens.

It can also be shown that spherical aberration causes a point source to be imaged as a disc of radius d_s given by

$$d_s = C_s f \alpha^3,$$

where f is the focal length of the objective lens, and C_s a coefficient measuring the spherical aberration. α has the same meaning as above.

If the numerical values applying to the lenses of the present instrument are substituted, it is found that

$$d_s = d_d = 9 \text{ A.}$$

when $\alpha = 4.2 \times 10^{-3}$ radians.

Under these conditions, the broadening of the image (error) due to spherical aberration and diffraction combined is close to its minimum, and for many purposes this value of α may be regarded as a good compromise between the opposing requirements for minimum diffraction error and minimum

---

*The term "disc" is used in Section (iv) to denote a small area of almost uniform electron intensity, which falls off rapidly at the edges. The diameter of such a disc is therefore chosen somewhat arbitrarily.

spherical aberration error.

Following a suggestion by von Ardenne (1940[38]) that the various errors may, as a first approximation, be combined geometrically, the combined error due to spherical aberration and diffraction is given by

$$d_{s,d}^2 = d_s^2 + d_d^2 .$$

The resolving power is therefore limited to about 13 A. on the assumption that all errors due to causes other than spherical aberration and diffraction are negligible by comparison. It is now necessary to examine to what extent this is realised in practice.

Errors due to Chromatic Aberration.- Chromatic aberration is not reduced by limiting the angular aperture of a lens, and electromagnetic electron lenses have not been corrected for chromatic aberration. It has, however, been possible to reduce the errors due to chromatic aberration by using a highly monochromatic beam of electrons.

Variations in the wavelength associated with the electrons may arise as a result of fluctuations in the accelerating potential, and as a result of inelastic scattering. Fluctuations in the accelerating potential need not be so large as to affect the resolving power, because electron sources can be made to be monochromatic to a higher degree than light sources, owing to the great stability attainable in modern high tension supplies.

Chromatic aberration operating on electrons scattered inelastically affects the distribution of electron intensity in the image (p. 25), but does not greatly reduce the resolving power, provided that only a small proportion of electrons is scattered inelastically. This condition is essential for obtaining electron micrographs of good contrast and high resolution (p.34f.).

Fluctuations in the lens current supplies result in changes in focal length, with a consequent blurring of the image. This error, and that due to fluctuations in the high tension supply, will be estimated later (p. 32f.).

Errors due to Field Aberrations.- The field aberrations (coma, curvature of field, astigmatism, distortion, and the chromatic difference in magnification and rotation) vanish at the centre of the field, but become important for image zones at some distance from the electron-optical axis. These aberrations can be minimised by a suitable choice of lens constants, and by using a suitable combination of lenses. Zworykin et al. (1945, pp. 208 - 213) have discussed their effect on the resolving power of a two-stage electron microscope, and Hesse (1948) has applied Southwell's relaxation method to the design of the lenses constructed for the three-stage instrument in this laboratory.

The Attainment of High Resolution.- Under favourable conditions, a number of workers have reported values of about

20 A. for the resolving power of their instruments. This value is considerably in excess of the limitation imposed by the errors due to spherical aberration and diffraction (10 - 13 A.). Hillier & Ramberg (1947) showed that the residual astigmatism of the objective was the cause of this discrepancy. They described an ingenious method for correcting this aberration, and obtained a resolution of about 10 A.

Some further points arising in the design and operation of electron microscopes will now be discussed briefly with special reference to the present instrument.

The mechanical stability of the instrument is of the utmost importance, since any movement in the object plane is magnified by the overall magnification in the image plane. In addition, the lenses must remain accurately in alignment on the electron-optical axis while the instrument is in use, since imperfect alignment increases the errors due to the field aberrations.

The lens pole pieces, especially those of the objective, must be kept clean and free from scratches, since aberrations will be introduced by any lack of symmetry.

The electron source should be small and circular, and should give rise to an intense and homogeneous pencil of electrons of a divergence that can be varied by means

of the condenser lens. The shape and size of the source (as imaged at the specimen) determines the resolution of the diffraction pattern, since the diffraction maxima are images of the source (pp. 9, 10).

The intensity and the divergence of the beam determine the accuracy of visual focussing. The importance of adequate intensity is self-evident, and the question of how the divergence of the beam determines the resolving power and the depth of focus will now be discussed. Consider an illuminating beam of divergence α_c. Let the divergence of the image forming beam after leaving the specimen be α_o. Then α_o is greater than α_c by an amount depending on the nature of the scattering due to the specimen. With an uncorrected lens system, α_o should be as small as possible in order to reduce spherical and certain other aberrations. But α_o can be reduced, inter alia, by reducing α_c, which should therefore be a minimum to obtain the optimum resolving power. Finally, a simple calculation shows that the depth of focus of a lens system of angular aperture α is inversely proportional to $\tan \alpha$.

It is therefore evident that visual focussing should be carried out at or near critical illumination, i.e. with a strongly divergent illuminating beam, and hence when the depth of focus is small; whereas the exposure should be made after defocussing the condenser, i.e. with an almost parallel illuminating beam, ~~i.e.~~ and hence when the depth of focus is large. A

focussing aid based on this principle has been described by Le Poole (1947).

Chromatic aberration due to unstable electrical supplies.- Lack of stability in the electrical supplies may arise in three ways. Firstly, through slow drift during the time of exposure due to faulty components or contacts; secondly, through brief fluctuations in the mains supply; and thirdly, through ripple due to inadequate filtering and stabilisation. All three reduce the resolving power in the same way, but ripple is most important, since it acts continuously.

It can be shown that as a result of a change in potential ΔV in the accelerating potential V, a point source will be imaged as a disc of diameter d_c, given by

$$d_c = C_v f_o \alpha_o \frac{\Delta V}{V} ,$$

where α_o is the angular aperture and f_o the focal length of the objective lens. C_v is a coefficient depending on the chromatic aberration of the lens. If the maximum permissable error due to the chromatic aberration of the objective lens is considered to be 9 A., i.e. the same value as the errors due to spherical aberration and diffraction, the high tension supply must not vary by more than two parts in 10^5 (for $\alpha_o = 4.2 \times 10^{-3}$ radians, $C_v = 2$, $f_o = 0.6$ cm.).

Hillier & Vance (1941) reported a stability of four parts in 10^5 at a current drain of 0.5 mA. for the high

tension supply of an electron microscope developed by the Radio Corporation of America, Inc.

It can also be shown that as a result of a change of current ΔI in the objective lens current I, a point source is imaged as a disc of diameter d_I, given by

$$d_I = C_I f_o \alpha_o \frac{\Delta I}{I} ,$$

where α_o and f_o have the same significance as on p. 32, and C_I is a coefficient depending on the chromatic aberration of the lens. If the error due to a ripple in the objective lens current is also to be limited to 9 A., the lens current must not vary by more than three parts in 10^5 (for $\alpha_o = 4.2 \times 10^{-3}$ radians, $C_I = 1.5$, and $f_o = 0.6$ cm.) The stabilisation of the remaining lens currents is somewhat less critical.

(v) Resolution and Specimen Thickness.

The resolving power of the instrument constitutes a lower limit for the size of detail that can be resolved, but it does not follow that this limit will, in fact, be reached, even if the specimen exhibits detail of this order of fineness. The micrographs of zinc oxide crystals, a formvar replica of scratches on a glass surface, and a muscle fibril (Figs. 7, 8, and 9) were obtained under similar instrumental conditions, and indicate that the resolution

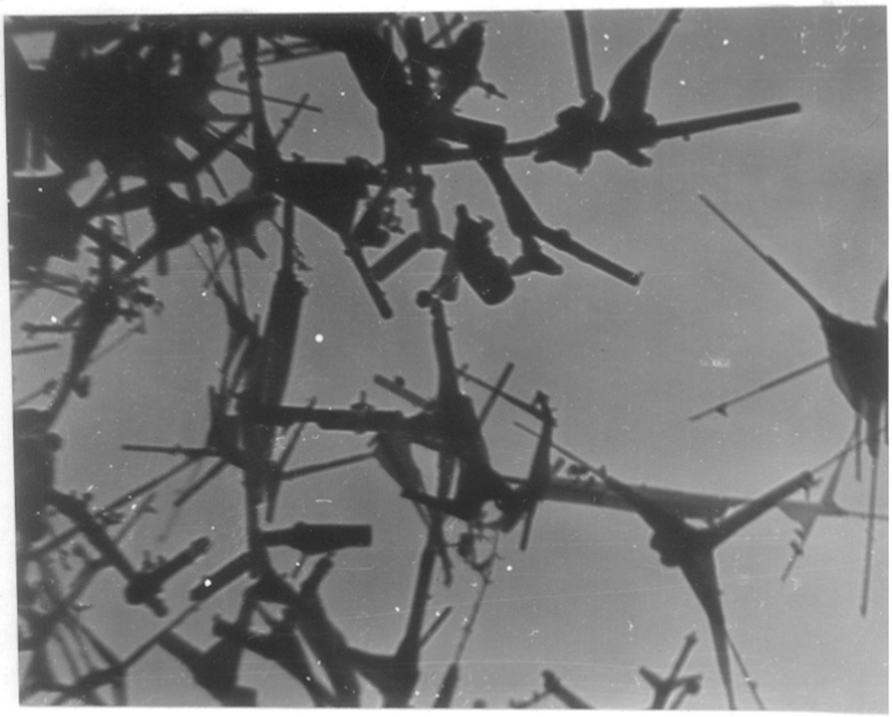

Fig. 7. Zinc oxide crystals. 30,000 x.

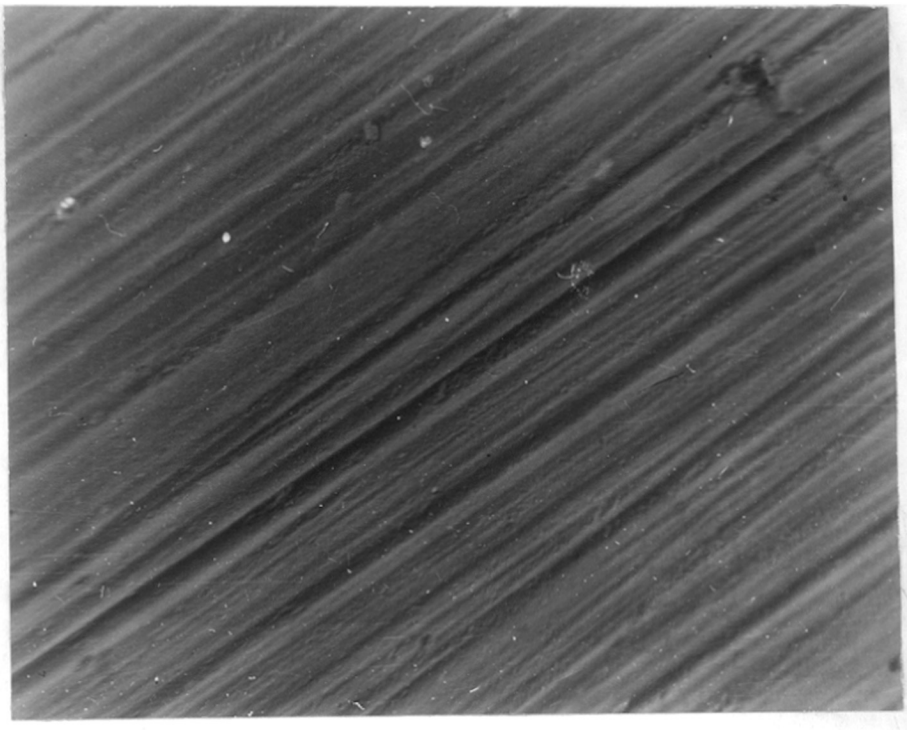

Fig. 8. Shadowed formvar replica of a scratched glass surface. 30,000 x.

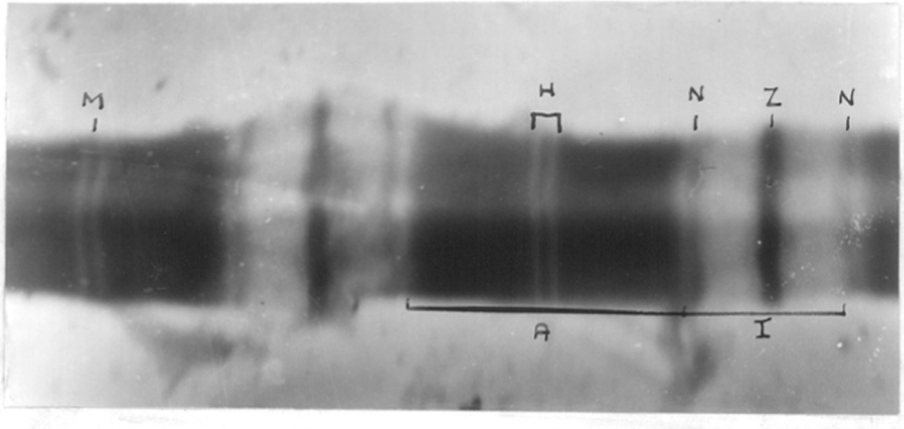

Fig. 9. Muscle fibril from rat rectus muscle. 30,000 x.

attained depends on the distribution of mass thickness within the specimen, as well as on the resolving power of the instrument.

The qualitative discussion of image formation given above permits neither the calculation of the maximum thickness of specimens that can be imaged in the electron microscope, nor the determination of the lateral or vertical resolution attainable.

Thin specimens.- In general, thin objects are suitable for examination. Contrast in the image arising from small differences in mass thickness of different parts of thin objects can be enhanced by staining or shadow-casting with heavy metals, by lowering the accelerating potential to about 50 kV, and by using suitable photographic materials. The value of a physical aperture in the objective lens will be discussed later, and the vertical limit of resolution will be discussed for a special case in connection with formvar replicas (p.54f).

Thick Specimens.- The problem of thick specimens has been treated quantitatively by von Borries (pp. 168 ff., 1949), who defined the "Aufhellungsdicke" (AD) of a specimen as the mass thickness of the object which on the average gives rise to a single elastic collision with every electron of the beam, i.e. a fraction of 1/e or 36.8 % of the electrons remain unscattered. If the proportion of scattered electrons

substantially exceeds this value, contrast becomes too low for satisfactory image formation, and the proportion of inelastically scattered electrons becomes excessive. A comparison with the few existing experimental data shows that the AD gives a useful practical guide to the thickness of objects which can still be imaged satisfactorily.

TABLE II

The AD of Carbon and Gold Specimens at different Accelerating Potentials.

Accelerating Potential (kV)	AD of Carbon ($gm.cm.^{-2}$)	AD of Gold ($gm.cm.^{-2}$)	Thickness of Carbon (A)	Thickness of Gold (A)
50	0.9×10^{-5}	0.5×10^{-5}	1500	260
100	1.6×10^{-5}	0.8×10^{-5}	2700	420
150	2.4×10^{-5}	1.2×10^{-5}	4000	630
200	2.6×10^{-5}	1.35×10^{-5}	4300	700

Note:- Density of carbon: 0.6 $gm.cm^{-3}$.
Density of gold: 19.3 $gm.cm^{-3}$.

Table II was compiled from the family of curves given by von Borries, and contains some values for carbon and gold as the scattering materials. The thickness of carbon specimens was calculated for a density of 0.6 $gm.cm^{-3}$, and can be used as a rough guide for organic specimens. Although the absolute values of the AD depend on the specimen material, the relative values at different accelerating potentials are similar for a

large range of substances, and show that it is worthwhile to increase the accelerating potential up to, but not much beyond, 150 kV.

Objective Apertures:- The other line of approach to the problem of increasing the contrast, especially of thick objects, is the use of a small physical objective aperture to eliminate the scattered electrons from the imaging beam. This is inconvenient for a number of reasons. The aperture must be kept scrupulously clean to prevent asymmetrical lens effects. It must be accurately centred, thus making the operation of the instrument more critical. It must be very small (20 - 100 μ, depending on its position in the lens), in order to limit the angular aperture to the optimum value (about 5×10^{-3} radians). Finally, it has to be removed to permit the examination of diffraction patterns on the final screen.

Hillier (1948) has shown that restricting the angular aperture to the optimum value increases the visibility of coarse, but not of fine detail, especially in thin objects, whereas the contrast of fine detail is increased at the expense of the resolving power by using angular apertures one order of magnitude smaller.

Various methods of overcoming the practical difficulties have been described. Hillier (1949) has used a double objective lens for obtaining low angular apertures

by means of comparatively large physical apertures (50μ). Haine, Page, and Garfitt (1950) describe a special intermediate section developed for the Metropolitan-Vickers(E.M.3) electron microscope, which permits the external centring and the easy removal of the aperture when it is not required. Dawson (1950) developed a simple attachment to the Siemens electron microscope permitting the external centring of the aperture by means of the specimen stage.

An objective aperture has been used by the majority of workers to increase the contrast of both thick and thin objects, and it is only necessary to refer to Wyckoff's work (1949) for the excellent results achieved. In one of the few cases, however, when the maximum operating voltage was raised to 400 kV, and objective apertures of suitable dimensions were used at the same time, an accelerating voltage of as much as 350 kV helped to improve the definition of fine detail in a thick object (Van Dorsten, Oosterkamp, & Le Poole, 1947).

(vi) The Present Instrument

The instrument in this laboratory was substantially in its present form in 1949, and it was felt that a period of continuous operation was desirable before making any major changes in its construction. The best resolution that could be attained approximated closely to the limitation imposed by the stability of the high tension supply. The basic features

of the design were found to be justified in the light of experience, but it soon became apparent that an improvement in the mechanical design of some of the parts was essential for reasonable ease in operation.

As a first step, a number of sections were re-built to reduce the chance of leaks by avoiding soldered joints under mechanical stress wherever possible, and by using soldered screw threads whenever such joints were unavoidable.

The alignment of the instrument was made easier by dispensing with the pump line between the manifold and the gun, and replacing it by a bye-pass for the condenser aperture (Fig.4).

It is now intended further to modify the instrument in the following respects.

The mechanical stability of the column will be increased by obtaining metal-to-metal contact at all vacuum joints along its length.

The gun will be re-designed on the lines of that used for the high voltage diffraction camera in this laboratory (Lewis 1950), both to increase the maximum accelerating voltage, and to improve the quality of the beam. At the same time, the movement needed for the alignment of the instrument will be improved with a view to making the adjustment more convenient.

The specimen stage will be re-designed, to obtain a

more positive movement, and to permit the insertion of an objective aperture.

The ripple in the high tension supply will be reduced by increasing the capacity of the output condenser, if and when this is justified by the reliability and ease of operation of the instrument.

4. THE ELECTRON DIFFRACTION CAMERA.

Description of the Apparatus.

The electron diffraction camera is the logical development of Thomson and Reid's method (1927) of demonstrating the wave nature of the electron. The Thomson-Fraser camera (1930) employed two small diaphragms in succession to collimate the electron beam, and could be used to obtain reflection and transmission patterns.

The Finch type camera (Finch & Quarrell, 1933) used in this laboratory is shown diagrammatically in fig. 10, and is remarkable for the simplicity of its mechanical design. The discharge tube is maintained at a pressure of about 10^{-2}mm of mercury by establishing equilibrium between the pumping speed and the leak rate. The leak rate is controlled by the pressure in a reservoir from which a capillary tube of suitable dimensions leads into the discharge chamber.

The beam enters the main body of the camera (maintained at 10^{-5} mm. Hg) through a small anode diaphragm, and is focussed on the final screen by an electromagnetic lens. The tilt of this lens can be varied, and this serves to deflect the beam, in order to scan different parts of the specimen. The non-axial use of the focussing coil has two further desirable consequences. Heavy ions are not brought to a focus along with the rest of the electron beam, and

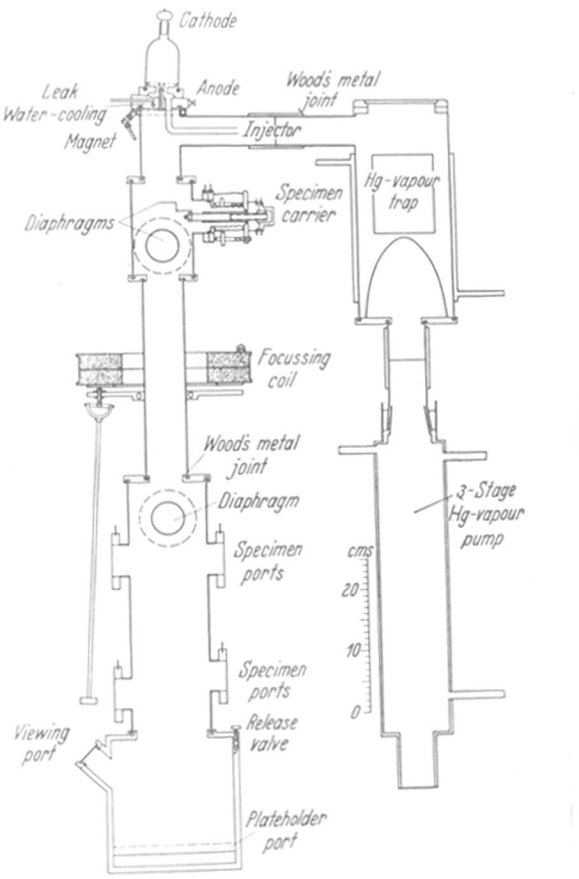

Fig. 10. Diagram of a Finch type electron diffraction camera.

electrons which have been slowed down by collision with the gaseous ions in the discharge tube diverge from the main focussed spot and give rise to a "tail", which can be eliminated by a second diaphragm just above the specimen. The specimen holder allows the specimen to be moved into any desired position. Two specimen ports are available for the insertion of the specimen holder, so that two camera lengths can be employed. At the long camera length the area near the central spot is enlarged, whereas at the short camera length a greater part of the pattern falls on the final screen.

The output of the high tension set is fed to the discharge chamber through a saturated diode. This arrangement ensures a constant current supply, and if the gas pressure in the discharge chamber is kept constant, the accelerating potential is also constant.

The use of a cold cathode discharge limits the accelerating potential to below about 70 kV; for work at higher potentials a hot cathode electron source is used.

The pumping system is similar to that of the electron microscope, but in some models the discharge chamber is pumped out by a separate oil diffusion pump in order to improve the vacuum in the main body of the camera.

The patterns can be recorded photographically by removing the fluorescent screen from the path of the electrons. Ilford Special Rapid plates are used for this purpose.

5. A COMPARISON OF MICROGRAPHS OBTAINED FROM THE SAME SPECIMEN BY DIFFERENT FORMS OF MICROSCOPY.

(i) Normal and Phase Contrast Illumination.

An epithelial cell taken from saliva is shown in figures 11 and 12 by normal and by phase contrast illumination, respectively. The contrast between different parts of the cell, and between the cell and its surroundings, is greatly improved by using phase contrast illumination. Fig. 13 shows the same contrast as is obtained by using normal illumination with a circular source. It was obtained by using an objective without a phase shifting annulus in its back focal plane, but with the same annular source as the phase contrast micrograph. It is therefore evident that the improvement resulting from the use of phase contrast illumination is not due to the employment of an annular source.

(ii) Optical and Electron Microscopy.

As a preliminary step to the work on scratches on glass surfaces, it seemed desirable to compare the micrographs obtained with different types of illumination in the optical microscope, and with shadowed and unshadowed replicas in the electron microscope.

A number of parallel scratches were ruled on a glass slide by means of a diamond point, which travelled over the

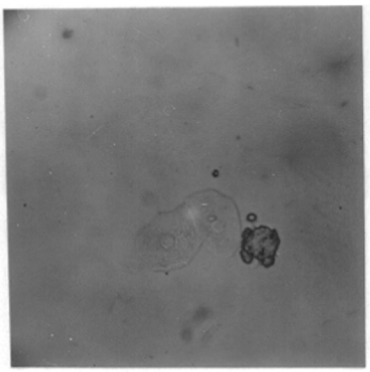

Fig. 11. Epithelial cell from saliva, by normal illumination, using a circular source. 140 x.

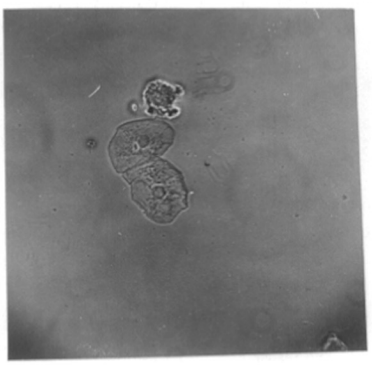

Fig. 12. The same epithelial cell by phase contrast illumination, using an annular source. 140 x.

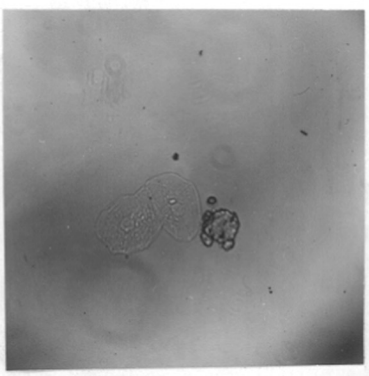

Fig. 13. The same epithelial cell by critical illumination, using an annular source. 140 x.

surface in two opposite directions. When the slide was examined by transmitted light and normal illumination, the scratches could not be observed. The scratches became visible by phase contrast illumination with transmitted light (fig. 14), owing to the difference in optical path in air as compared with glass, but contrast was still insufficient with a high power objective. The scratches could be clearly observed even under a high power objective when examined with incident light, especially after vacuum deposition of a thin layer of silver on the surface to increase its reflectivity (fig. 15). The scratches appeared as two separate lines each about 1000 A. in width (total width about 2000 A.). This is well below the limit of resolution of a 4 mm. objective (about 4000 A.). The scratches made by the two directions of travel of the diamond point could not be distinguished from each other.

Formvar replicas of the same surface were made, and examined by electron microscopy (fig. 16). Shadowing with gold-manganin (in the ratio of 1 : 1) was employed to enhance the contrast (figs. 17 and 18). Two different groups of scratches, corresponding to the two directions of travel, could now be distinguished, and were each found to be composed of two major components, which were further differentiated and about 2000 A. in width, and a number of single scratches,

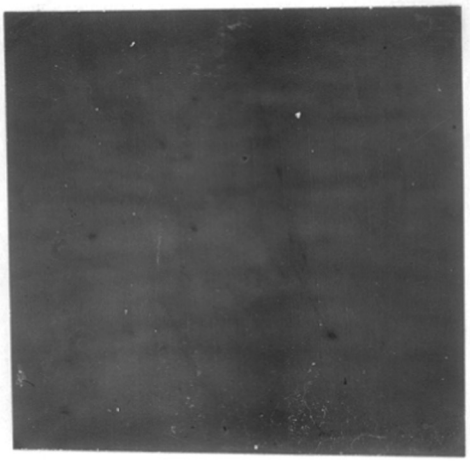

Fig. 14. Scratches on glass made by means of a diamond point, by phase contrast illumination. 75 x.

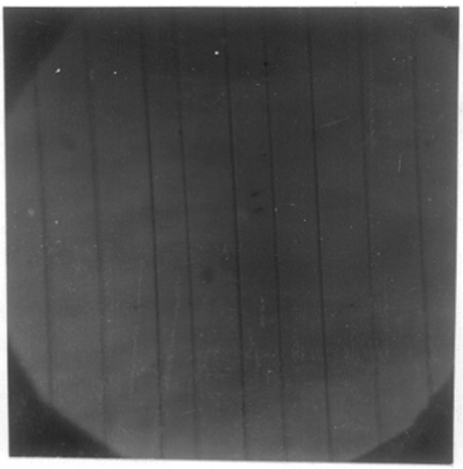

Fig. 15. The same scratches as in fig. 14, but silvered in vacuo, and by vertical illumination. 315 x.

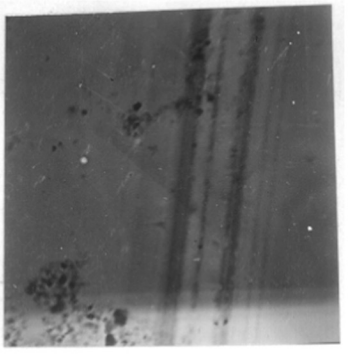

Fig. 16. Formvar replica of a scratch on glass. 10,000 x.

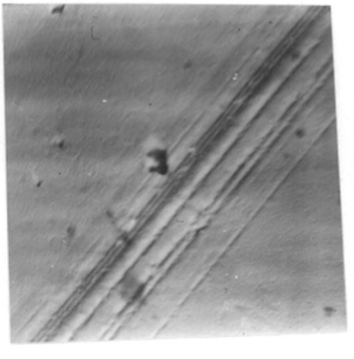

Fig. 17. Formvar replica of the same scratch on glass as fig. 16, but shadowed. 10,000 x.

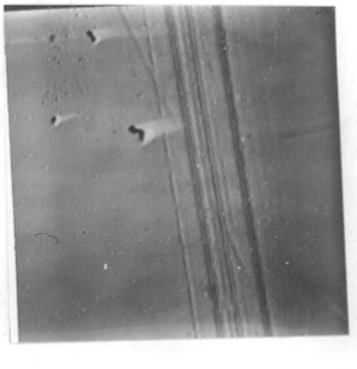

Fig. 18. Shadowed formvar replica of a scratch ruled in the opposite direction from the one shown in fig. 17. 10,000x

about 400 A. in width. The width of the two groups of scratches was 3500 A. and 5000 A.

A comparison of the width of the scratches obtained by measurment of the optical and the electron micrographs shows that the electron microscope detects differences in surface level of small lateral extent not detected by the optical microscope. The greater resolving power of the electron microscope is clearly demonstrated by the greater amount of detail which it reveals.

II. THE APPLICATION OF THE INSTRUMENTS.

1. The Scratching and Polishing of Glass Surfaces.

(i) The Beilby Layer.

Newton (1704) thought that polishing consisted of wearing away the projections on the surface by "grating and fretting" until the projections could no longer be distinguished. Rayleigh (1901) suspected that polishing occurred on a molecular scale. Beilby's views on polish, based on an extensive series of experiments, are probably best summed up in his own words (1921):-

"(1) In every one of these substances, if it is sufficiently homogeneous to be polished at all, the fundamental principles on which polishing depends are absolutely identical."

"(2) The polished surface in a solid substance is as truly due to the presence of a surface tension skin as is the surface of a liquid."

By means of the optical microscope, Beilby observed the disappearance of scratches on a wide variety of surfaces as a result of polishing, and found that they re-appeared on etching. He concluded that the scratches had been filled in by material which had flowed from other parts of the surface, and that the etchant attacked this material preferentially. He suggested that the flowed material was

amorphous as a result of the rapid cooling on cessation of the local heating caused by the polishing action.

In polishing metallic surfaces, Bowden & Ridler (1936) were able to show that temperatures approaching that of the melting point of the material were attained locally. Beilby's hypothesis in the case of metals has been further confirmed by a remarkable observation. Finch, Quarrell, & Roebuck (1934) found that the Beilby layer on a polished copper surface was able to dissolve zinc crystals at room temperature, and that this property was not exhibited by the crystalline surface. Finally, Finch, Quarrell & Wilman (1935) found that the thickness of the Beilby layer depended on the vigour of the polishing action.

The Beilby layer on various calcite cleavage faces has been studied by electron diffraction and also by means of epitaxy (as orientated overgrowths were called by Royer, 1928). Finch (1937) obtained halo patterns from polished calcite faces steeply inclined to the cleavage planes, whereas cleavage surfaces or crystal faces cut close to one of the cleavage planes gave Kikuchi line patterns even after vigourous polishing. It was also found that heating the Beilby layer on faces strongly inclined to the cleavage planes resulted in Kikuchi line patterns being obtained. Finch considered that an amorphous Beilby layer was formed by

polishing, and immediately re-crystallised on faces cut close to the cleavage planes, but re-crystallised only after heating on faces steeply inclined to the cleavage planes. This view was further supported by Finch and Whitmore's (1938) experiments, in which sodium nitrate crystals were grown on similar polished calcite faces. Sodium nitrate crystals grew epitaxially on all heated calcite faces which gave Kikuchi line patterns, but were random on those surfaces which gave halo patterns.

Beilby (1921) had made similar observations with epitaxial overgrowths, and regarded them as evidence for atomic forces exerted by the crystalline substrate acting through the comparatively thick (and amorphous) Beilby layer. This explanation is untenable in view of the rapid decrease of these forces with distance, and therefore these experiments on epitaxy must be regarded as a striking confirmation of Finch's earlier electron diffraction results.

Leise (1948) claims to have obtained Kikuchi line patterns on polished calcite faces irrespective of their inclination to a cleavage plane, but this could, perhaps, be explained by insufficient polishing. Raether (1948) was unable to repeat the dissolution of zinc by polished copper surfaces (Finch, Quarrell & Roebuck, 1934). He used both copper and polished steel as substrates, and ascribed the

disappearance of the zinc pattern to surface contamination rather than the properties of the Beilby layer. Raether also believes that the Beilby layer is not amorphous, but consists of very small crystals rubbed off the surface during polishing, and while it must be admitted that the electron diffraction patterns obtained from amorphous material and from very small crystallites are indistinguishable, it is difficult to see how the indisputable phenomenon of surface flow can be accounted for by small crystallites rubbed off the surface.

Glass yields broad halo patterns both before (Maxwell & Mosley, 1935) and after (Kamogawa, 1940) polishing, and was therefore chosen as a convenient material for studying the behaviour, but not the structure, of the Beilby layer.

(ii) Previous Work on Glass Surfaces.

Beilby (1921) observed flow on glass surfaces, and found that the skin formed as a result of fire glazing offered more resistance to grinding than the succeeding layers. He concluded that the flowed skin was harder than the bulk of the material. Golz (1943), in an electron microscopic study of the glass surface, found no structure in a fire glazed surface, but observed sleeks on polished surfaces. Marx, Klemm, and Smekal (1941) obtained tracks on glass surfaces made by steel needles. The tracks were found to be smooth and free from fractures, which was ascribed to

the absence of cracks (possibly similar to Griffith cracks, see Griffith, 1921) on a sufficiently fine scale to provide enough starting points for the development of fractures. These authors also estimated the amount of heat liberated under their experimental conditions, and found it sufficient to cause the glass to melt locally. Deacon, Ellis, Cross & Sennett (1948) tested the formvar replica method on glass surfaces, and observed that a sleek drawn across a second sleek wipes out the first. Custers (1949) observed chips and long turnings cut out of the surface during scratching. Finally, Brown (1949) confirmed the existence of surface flow on glass surfaces for scratches down to about 0.1 μ in width.

(iii) Scratches Examined by Optical Microscopy.

A Heavy Scratch made by a Carborundum Point.- A point of a carborundum crystal was drawn by hand across a microscope slide. The movement was jerky, and at several points large concoidal fractures were caused, which are shown in fig. 19. When the surface was silvered, and a micrograph was taken with incident light, a coloured area (shown darker on the print, fig. 20) could be distinguished around the large concoidal fracture. The straight portion of the scratch showed small ridges.

The Polishing and Etching of a Heavy Carborundum Scratch.- The heavy scratch was made in the same way as before, and

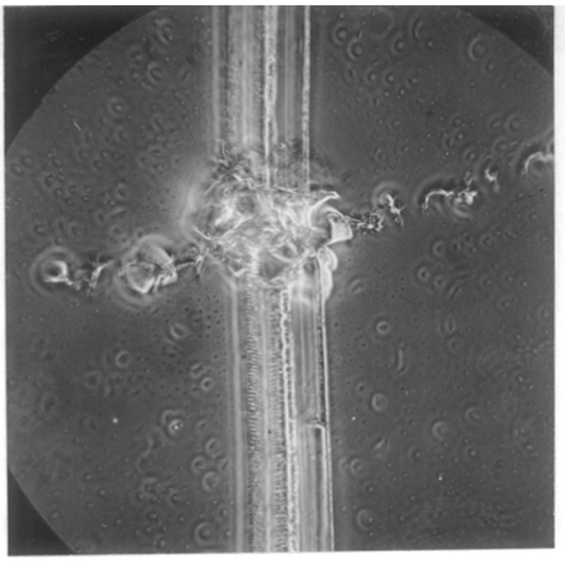

Fig. 19. Carborundum scratch on glass. 315 x.
Phase contrast illumination.

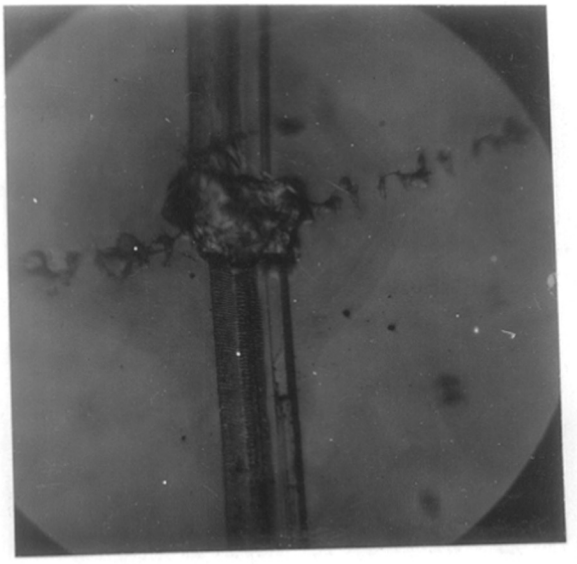

Fig. 20. The same scratch as fig. 19, but silvered in vacuo.
Vertical illumination. 315 x.

a diamond point was used to make a cross scratch which served to mark the position. The scratch was almost polished out by means of moist rouge, using one finger as a backing. Finally, the slide was etched in 1% hydrofluoric acid. Figs. 21, 22, 23 were taken at the three stages (original, polished, and etched scratch), and show that the scratch was almost obliterated by polishing; etching revealed a much greater degree of damage, both in depth and extent, than was discernible in and around the original scratch.

The Production, Polishing and Etching of Light Diamond Scratches.- In order to produce scratches suitable for examination in the electron microscope, a diamond point was mounted on a leaf spring which could be held in the tail stock of a lathe, and the glass slide was clamped on the carriage. By this arrangement, a grating could be ruled on the glass slide, with the diamond point travelling in opposite directions for neighbouring scratches.

Two sets of lines (gratings) were ruled at different loads, and at a small angle to one another, in order to provide reference marks after the lighter set had been polished out. The original gratings (1000 lines per inch) were examined over their entire width, and the scratches ruled at the same load, and in the same direction of travel, were found to be similar. Figs. 24, 25 and 26 show, respectively, the original gratings,

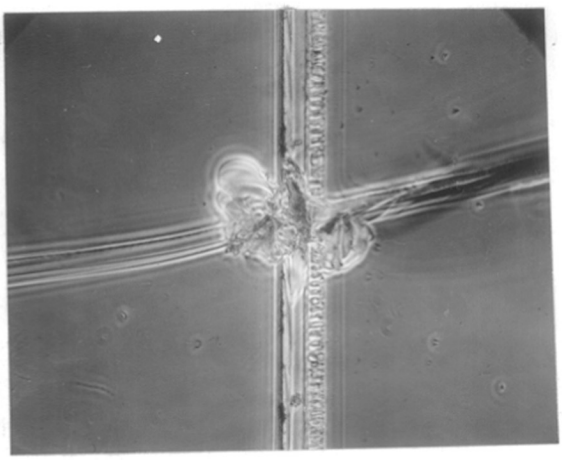

Fig. 21. A coarse diamond scratch on glass, by phase contrast. 315 x.

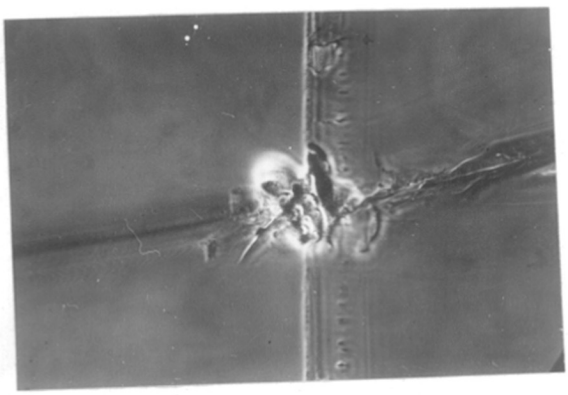

Fig. 22. The same scratch as fig. 21, after polishing with moist rouge. By phase contrast. 315 x

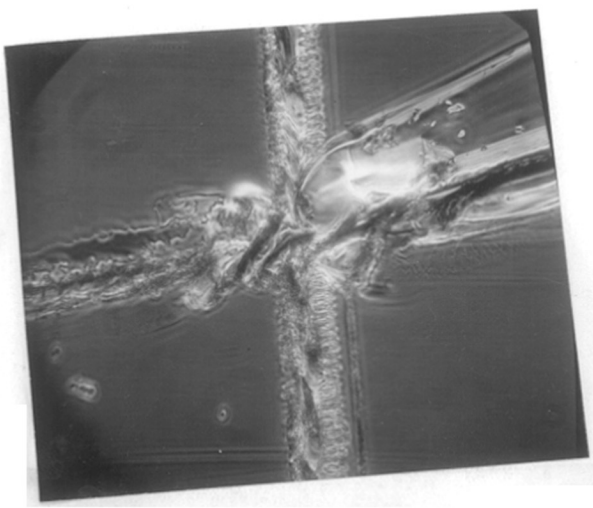

Fig. 23. The same scratch as fig. 21, after polishing and etching. By phase contrast. 315 x.

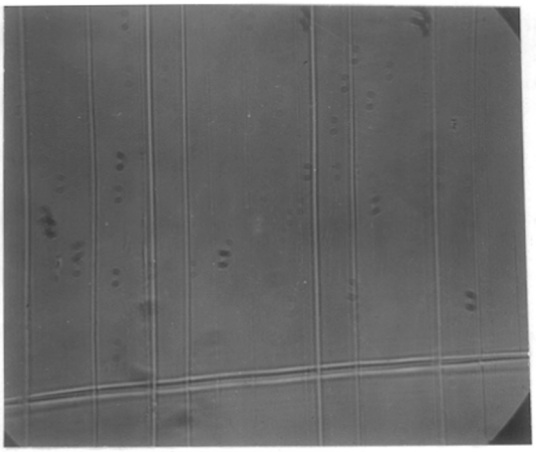

Fig. 24. Two gratings consisting of fine diamond scratches ruled on glass. By phase contrast illumination. 315 x

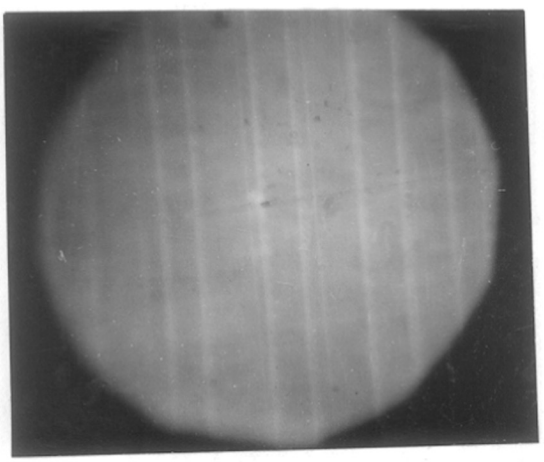

Fig. 25. The same gratings as fig. 24, after polishing. By vertical illumination. 315 x.

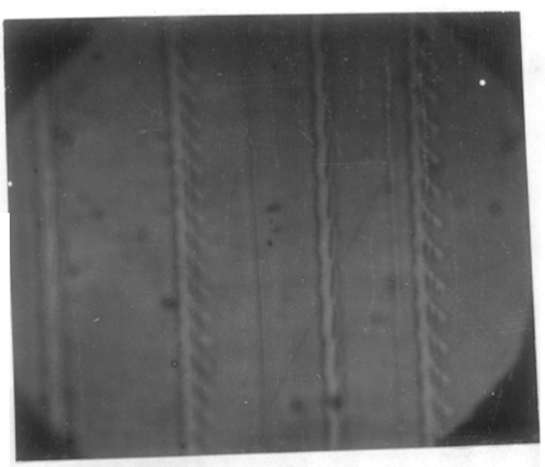

Fig. 26. The same gratings as in fig. 24, after polishing and etching, silvered in vacuo. By vertical illumination. 940 x.

after nearly polishing out the lighter grating with rouge, and after etching. The observations concerning the effect of polishing out and etching are similar to those recorded in the previous sub-section, except that etching did not reveal a more extended area of damage.

The Efficacy of the Replica Method.- Figs. 27 and 28 show the same carborundum scratch on glass on the surface of the glass slide and on a formvar replica, respectively. The replica shows the same detail as the surface itself, but the cross scratch is slightly bent instead of being straight, indicating some large scale distortion of the replica.

(iv) The Polishing Powders

The following three polishing powders were used in the course of this work:-

(1) Jeweller's Rouge.

(2) "Diadust" (A diamond dust containing no particles greater than 1 μ in diameter).

(3) Elutriated diamond dust.

Figs. 29, 30 and 31 were obtained by putting a drop of an aqueous suspension of rouge, diadust or elutriated diamond dust on a formvar film, which was examined in the electron microscope after allowing it to dry. Rouge (fig. 29) was badly dispersed, but wherever individual particles can be discerned, they are roughly spherical, and about 1 μ in diameter. Diadust (fig. 30) contains many similar particles

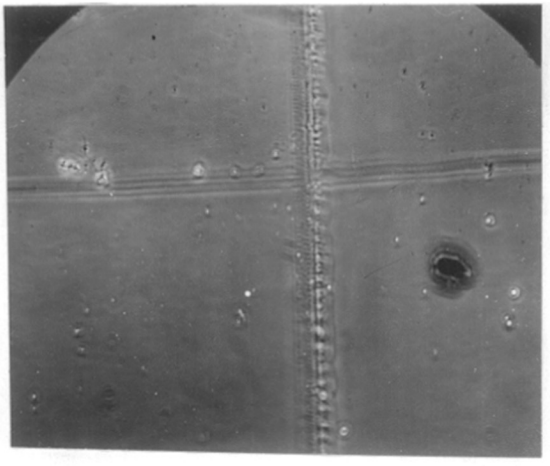

Fig. 27. Carborundum scratch on glass. By phase contrast illumination. 315 x.

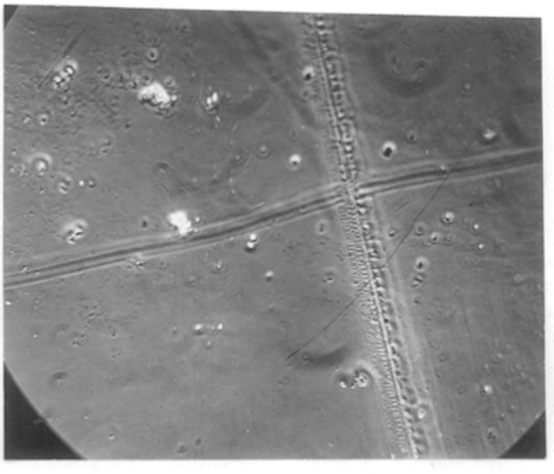

Fig. 28. Formvar replica of the same scratch. By phase contrast illumination. 315 x.

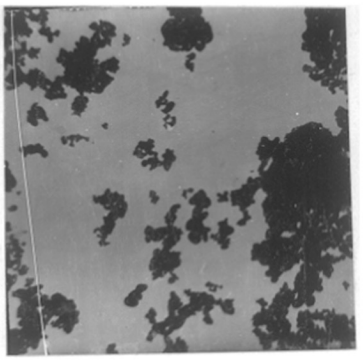

Fig. 29. Jeweller's rouge suspended in water and allowed to dry, by electron microscopy. 5000 x.

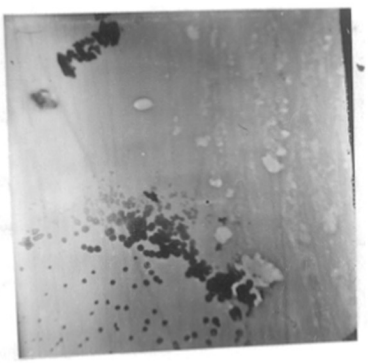

Fig. 30. "Diadust" suspended in water and allowed to dry, by electron microscopy. 5000 x.

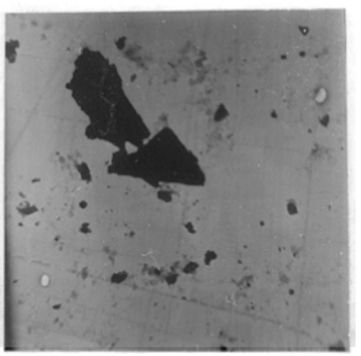

Fig. 31. Elutriated diamond dust, suspended in water and allowed to dry, by electron microscopy. 5000 x.

which are well- dispersed, as well as some particles up to 1 μ in diameter, and showing sharp edges and points. In the elutriated diamond dust (fig. 31) there are some small particles, as well as large particles up to 3 μ in diameter, again showing sharp edges and points.

Water, paraffin oil and vaseline were used as suspending media during polishing.

(v) The Treatment of the Glass Surfaces.

The Production of Scratches.- Two kinds of scratches were made. The first kind consisted of a grating made up of multiple scratches, and ruled as described on p. 50. Individual scratches could sometimes be identified in the electron microscope, and an extensive examination showed that alternate scratches were similar throughout the area covered by an electron microscope grid.

Scratches of the second kind were made by rubbing the surface with an unsuitable polishing powder suspended in water (elutriated diamond dust), and using the finger as a polishing pad, in the same way as for polishing.

Polishing.- Polishing was carried out at right angles to the direction of scratching. The vigour of the polishing action was judged by counting the number of polishing strokes, while endeavouring to keep the pressure constant.

Etching.- The slides were etched in approximately 1% hydrofluoric acid, until the working marks, which had been ob-

literated by the fire glaze, became visible.

The slides were washed in teepol and water before taking replicas.

(vi) The Replica Method.

A drop of a 0.2% solution of "Formvar" in dioxan was placed on the part of the slide to be examined, and allowed to drain and dry in a desiccator. The resulting film was stripped in water, and a grid placed on top of it. A microscope slide with a hole slightly larger than the diameter of the grid was used to pick up the replica in such a way that the grid was situated above the hole in the slide. After drying, this method permitted the examination of the replica in an optical microscope to check that the film was complete. Finally, the grid was removed from the slide by pushing it through the hole by means of a peg, and shadowed in a vacuum better than 10^{-4} mm. Hg. with gold-manganin (in the ratio 1:1) at an angle of about 1 : 5, with a thickness of about 10 A. on the flat portions of the replica, assuming that the shadowing metal had the same density on the replica as in the form of drawn wire.

The relation between the shape of the surface and the appearance of the image has been discussed by Brown (1949) and others. A scratch on the surface is represented as a dark line on a positive print, provided that the back

surface of the replica is flat, but the shape of this side of the replica depends on its thickness, and on the depth and extent of the surface detail. The thin replicas used in the present work did not show a flat back surface; this was verified by depositing on it a layer of silver about 1000 A. thick, and examining this surface by vertical illumination, when the scratches replicated by the front of the replica were still clearly visible. It must, however, be remembered that vertical illumination provides a very sensitive check on surface undulations. If the back of the replica follows the front perfectly (as is the case with aluminium oxide replicas), each scratch on the surface is represented by two dark lines on a positive print. Since many single dark lines were observed during the present work, it must be concluded that the replicas were not of uniform thickness, and that the replica of a scratch on the surface can be adequately represented by fig. 32.

Shadowing along a smooth scratch does not substantially affect its appearance in the micrograph. Shadowing across it produces a light line on a positive print as a result of the smaller thickness of shadowing metal on the side away from the source, and a dark line on the opposite side, because of the greater thickness of shadowing metal.

Deacon et al. (1948) have estimated that thin form-

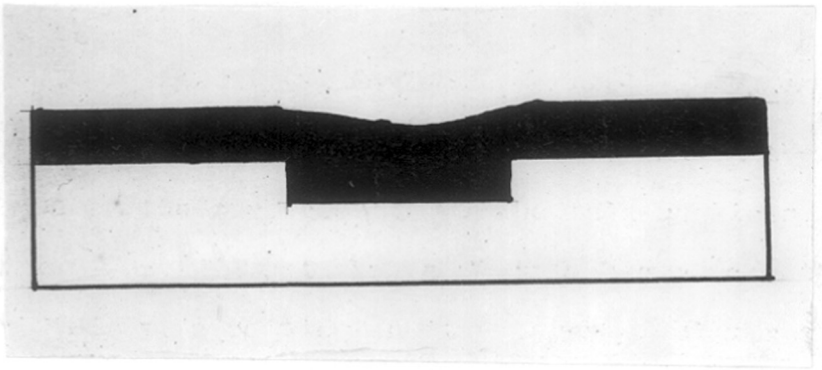

Fig. 32. Diagram of the cross-section of a formvar replica (shown in black) of a scratch on a glass surface (shown in white).

Fig. 33. Shadowed formvar replica of scratches on a glass slide, made by rubbing with elutriated diamond dust, by electron microscopy. 10,000 x.

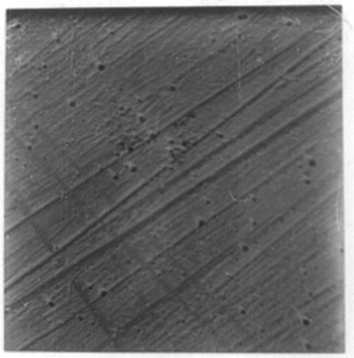

Fig. 34. Shadowed formvar replica of the same surface after etching with 1% hydrofluoric acid, by electron microscopy. 10,000 x.

var replicas give accurate representations of detail down to 200 - 500 A., but when shadowed obliquely were able to detect detail of a lateral extent of 100 A., and a height of 50 A. The best lateral resolution obtained during the present work was estimated to be 170 A.(fig. 8), and the shortest shadow length was 150 - 200 A., which may correspond to a difference in level of 30 - 40 A. The uncertainty arises because the inclination of the surface on which the shadow falls is not accurately known.

(vii) Experimental Results Obtained with the Electron Microscope.

The experimental results will be presented in the form of a table, which should be read in conjunction with the micrographs shown in figs. 16 - 18 and 33 - 47.

TABLE III

No. of Slide.	Treatment of Surface.	Micrographs and Comment.	Conclusions.
1.	Scratched by rubbing with elutriated diamond dust suspended in water.	Fig. 33.	Flowed material is associated with each scratch, and is removed preferentially by the etchant.
	Etched.	Fig. 34. The scratches have become broader and deeper.	

No. of Slide.	Treatment of Surface.	Micrographs and Comment.	Conclusions.
2.	Scratched by ruling with a diamond point.	Figs. 16 - 18.	Polishing is accompanied by general surface flow, no individual polishing marks being visible. The flowed material fills in the large irregularities, but the detail becomes part of the flowed layer. Etching removes the flowed layer preferentially, and reveals again those marks which have only been filled in by polishing.
	Polished with rouge suspended in water.	Fig. 35. The scratches have almost disappeared, but no polishing marks can be seen.	
	Etched.	Fig. 36. The scratch has re-appeared, but has changed in detail.	
	Re-polished with rouge suspended in water.	Fig. 37. The scratch has again nearly disappeared, but polishing marks can be discerned.	The re-appearance of a filled-in scratch does not depend on the removal of flowed material associated with the scratching action. The etched surface appears to be softer than the fire glazed surface.
	Etched.	Fig. 38. The main body of the scratch has re-appeared.	
3.	Scratched as slide 1.	Similar to fig. 33.	The polishing was so vigourous that the scratches became part of the flowed layer, and could therefore not be uncovered by etching.
	Heavily polished with rouge suspended in water.	Fig. 39. The scratches have been obliterated.	
	Etched.	Fig. 40. Only a few polishing marks appear.	

No. of Slide.	Treatment of Surface.	Micrographs and Comment.	Conclusions.
4	Scratched as slide 2.	Fig.41.	This polishing powder does not produce general flow, but only localised flow associated with the individual tracks of the diamond particles. There may be some abrasion.
	Polished with elutriated diamond dust suspended in water.	Fig.42. The scratch has become fainter, and is wiped out in some places by the polishing tracks.	
	Etched.	Fig.43. The scratch has become coarser, and numerous polishing marks appear.	
5	Scratched as slide 1.	Similar to fig. 33.	The action of this polishing powder is intermediate between that of rouge and that of elutriated diamond dust.
	Polished with diadust suspended in water.	Fig.44. The scratches have almost disappeared, and some polishing marks are visible.	
	Etched.	Fig.45. The scratches have re-appeared, and few polishing marks are visible.	

No. of Slide.	Treatment of Surface	Micrographs and Comment.	Conclusions.
6	Scratched as slide 1.	Similar to fig.33.	This polishing powder when suspended in paraffin is almost as good as rouge suspended in water.
	Polished with diadust suspended in paraffin oil.	Fig.46. The scratches have almost disappeared, and few polishing marks are visible.	
	Etched.	Fig.47. The scratches have re-appeared, and a few polishing marks are visible.	

Rouge, elutriated diamond dust and diadust were each tried as polishing powders suspended in water, paraffin oil and vaseline. There was no noticeable difference in the polishing properties of each powder, except in the cases of diadust, which was more effective when suspended in paraffin oil (Table III, no. 6) or vaseline, and of rouge, which was less effective when rubbed out in vaseline.

Finally, the polishing effect of a finger dipped in water, paraffin oil, and vaseline was tried, and the result was negative.

ELECTRON MICROGRAPHS OF SHADOWED FORMVAR REPLICAS

The original scratches were similar to those shown in figs. 16 - 18.

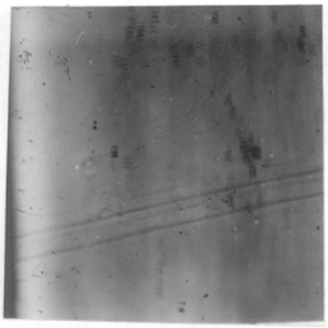

Fig. 35. A scratch after polishing with rouge.
5000 x.

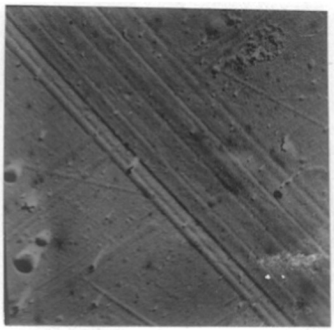

Fig. 36. A scratch after polishing and etching.
10,000 x

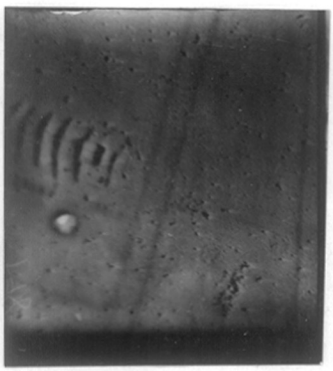

Fig. 37. A scratch re-polished with rouge after etching.
5000 x

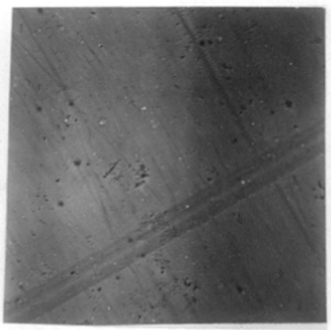

Fig. 38. A scratch after re-polishing and re-etching.
5000 x

ELECTRON MICROGRAPHS OF SHADOWED FORMVAR REPLICAS.

Slide 3.

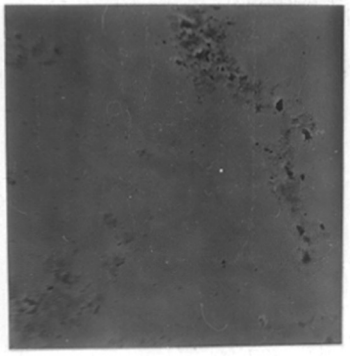

Fig. 39. A surface heavily polished with rouge. 5000x.

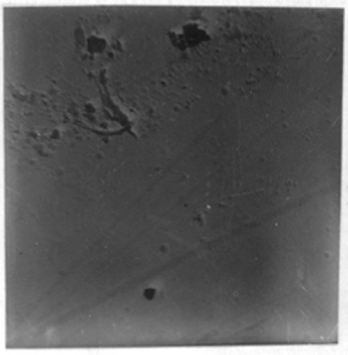

polishing marks.

Fig. 40. The surface shown in fig. 39, after etching. 10,000 x.

Slide 4.

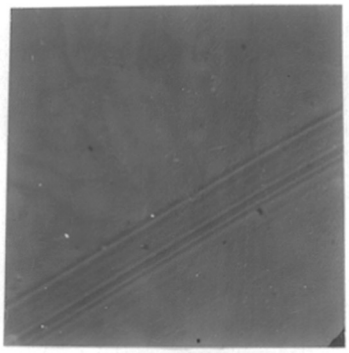

Fig. 41. A scratch on a glass surface. 10,000 x.

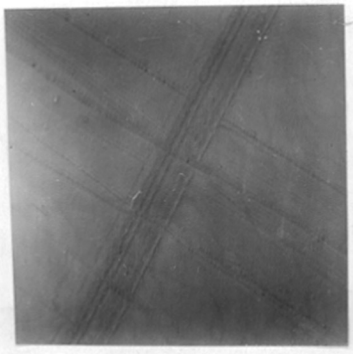

Fig. 42. A scratch similar to that shown in fig. 41, after polishing. 10,000 x.

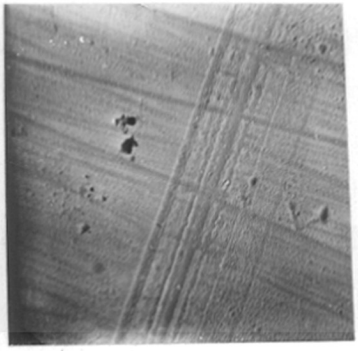

Fig. 43. A scratch similar to that shown in fig. 41, after polishing and etching. 10,000x.

ELECTRON MICROGRAPHS OF SHADOWED FORMVAR REPLICAS.

Slide 5.

scratches

polishing marks.

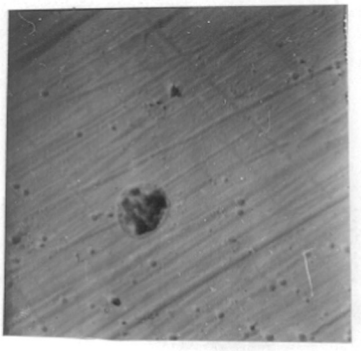

Fig. 44. Scratches originally similar to those shown in fig. 33, after polishing Zn with diadust suspended in water. 10,000x.

Fig. 45. The surface shown in fig. 44, after etching. 10,000 x.

Slide 6.

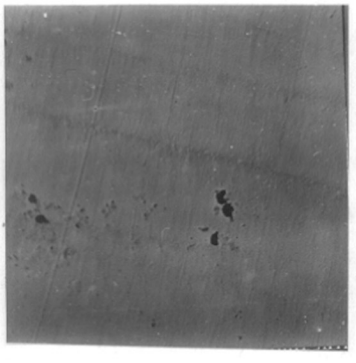

scratches

polishing marks.

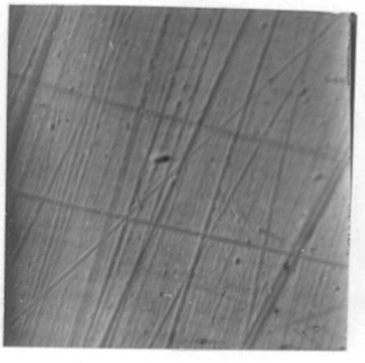

Fig. 46. Scratches originally similar to those shown in fig. 33, after polishing with diadust suspended in paraffin. 10,000 x.

Fig. 47. The surface shown in fig. 46, after etching. 10,000 x.

(vii) Discussion.

A good polish can only be achieved by causing the material in the surface layer to flow by liquefying it locally. This flowed material gradually fills in any depressions on the surface, and the surface becomes level if the process is sufficiently vigorous. In this event, however, the depressions can still be uncovered by etching.

The vigour of the polishing action determines the thickness of the flowed layer, and when this thickness is greater than the depth of a particular depression in the surface, this depression becomes an integral part of the Beilby layer, and does not re-appear on etching.

The present work, done on the scale of the electron microscope confirms and extends Beilby's (1921) conclusions.

There was no positive evidence of abrasion when the polishing action was imperfect. In these cases the grain of the polishing powder, individually or in aggregates, caused only localised flow in the immediate vicinity of the polishing mark made by them, but failed to establish a continuous layer of flowed material over the surface. This mechanism is the same as that observed in making scratches - in both cases etching removed material from the immediate vicinity of the scratch or polishing mark more rapidly than from the remainder of the surface. It follows that all

intermediate stages between the two extremes of localised and general flow should exist in practice. On polishing glass with different polishing powders suspended in different media these were, in fact, realised.

The following explanation of the different behaviour of the three polishing powders is suggested. Generalised flow, or true polishing is caused by the smallest approximately spherical particles of the polishing powders (in all cases 0.1 μ). Jagged particles of 1 μ or larger merely make scratches, each being associated with localised flow. The best polish is achieved with rouge, which contains no large particles. Diadust gives a good polish disfigured only by a few polishing marks because the proportion of small to large particles is sufficiently high. Elutriated diamond dust gives a poor polish because the proportion of small to large particles is too low. The effect of the suspending medium is comparatively small.

2. THE STRUCTURE OF STRIATED MUSCLE IN DIFFERENT STATES OF ACTIVITY.

(i) Introduction.

The structure of striated muscle in different states of activity described in this section was carried out in collaboration with Mr. C. Sitaramayya of King's College, London. Most of the results have been described elsewhere as part of a wider study of diaphragm muscle (Bluhm and Sitaramayya, 1951), but it will now be treated as an application of the phase contrast and electron microscopes to biological tissues. Specimen preparation, interpretation of micrographs, and the information that can be obtained from them will be discussed, but no attempt will be made to present a full review of the biological background.

"The view which will be taken as a basis for discussion is that the (striated) muscle fibre is composed of a large number of myofibrils embedded in a viscous matrix of undifferentiated protoplasm or sarcoplasm, containing numerous nuclei, the whole being enclosed in a fine sheath, the sarcolemma. Each fibre receives a nerve supply, and is connected terminally to connective tissue and tendon fibres". This sentence is quoted from Barer's (1948) review entitled "The Structure of the Striated Muscle Fibre", to which

reference may be made for a balanced review of the present state of knowledge.

The appearance of the striations, and their function in muscular contraction, have been a subject of controversy for over 100 years, largely due to the smallness of much of the detail. It is not surprising, therefore, that striated muscle was examined in the electron microscope, in spite of the problems presented in specimen preparation.

The cutting of sections sufficiently thin for examination in the electron microscope is difficult and laborious (Richards, Anderson and Hance, 1942), but good results have been obtained with freeze-dried material (Pease and Baker, 1949). The simplest technique, so far only applied to fixed tissue, consists of breaking up the muscle into myofibrils, which are thin enough to be examined in the electron microscope, and at the same time represent an important functional unit of the muscle fibre. (Hall, Jakus and Schmitt, 1945; Beams, Evans, Jenny and Baker, 1949; Draper and Hodge, 1949).

As a result of this work with the electron microscope, and that with the optical microscope which preceded it, the myofibril can now be regarded as a roughly cylindrical tube divided into sarcomeres. Each sarcomere consists of two bands, A and I, differing in their absorption of light, their

birefringence, and their scattering power of electrons. The Z band (in the middle of the I band) is part of a continuous membrane linking the myofibrils together (Fig.48). Under suitable conditions, filaments are observed running along the length of the myofibril. They can almost certainly be regarded as actomyosin filaments (Szent-Györgi, 1946, and others). In mammalian muscle (though not in insect muscles), the H disc is very near, and the M and N lines are beyond, the limit of resolution by optical microscopy. The electron microscope reveals them clearly (Fig.9) in some tissues but not in others, and a number of conflicting suggestions, which will be discussed later, have been put forward to account for their presence or absence.

The relation between the appearance of H, M, and N and the state of activity was therefore studied in rat diaphragm muscle. At the same time, the lengths of the A and I bands of a number of individual myofibrils were measured in various states of activity, and any changes were compared with those previously observed in the whole muscle fibre under the optical microscope (Buchthal, Knappeis and Lindhard, 1936), and in some cases, with the earlier electron microscope work referred to above.

(ii) Experimental.

Specimen Preparation - Specimen preparation followed the method used by Hall et al. (1946), the essential steps being fixation in 10% formalin for 24 hours or more, dissociating the tissue in a 'Magimix' for ~4 minutes at 15,000 r.p.m., and finally centrifuging for ~5 minutes at 3,000 r.p.m. A drop of the resulting suspension was examined under the phase contrast microscope to ensure that the concentration of myofibrils was suitable and that the material was clean. This prevented the examination of weak or dirty material in the electron microscope, and so saved a great deal of time.

Another drop of the suspension was then mounted on a formvar coated grid, stained with phosphotungstic or phosphomolybdic acid to enhance the contrast, and allowed to dry. According to Draper and Hodge (1950), staining also stabilises the structure against incineration by the electron beam. Shadowing with gold-manganin (in equal amounts) was used only in a few cases to obtain an estimate of the thickness of the various bands of the myofibril, since it did not increase the amount of detail visible within the myofibril itself (Fig.49).

Material Examined - Relaxed diaphragms from six rats were compared, and no significant variation was found in the size

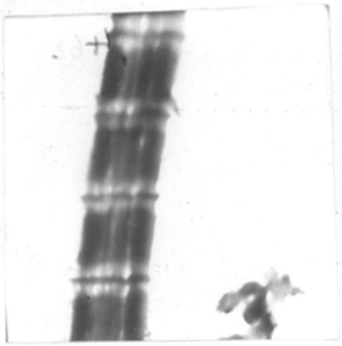

Fig. 48. Myofibril from rat diaphragm by electron microscopy. 5000 x.

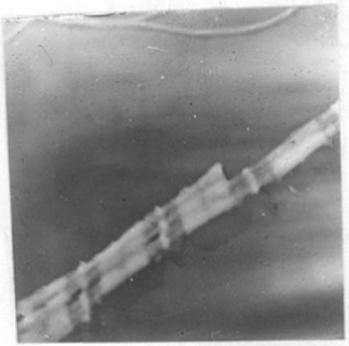

Fig. 49. Shadowed myofibril from rat diaphragm, negative print. 5000 x. By electron microscopy.

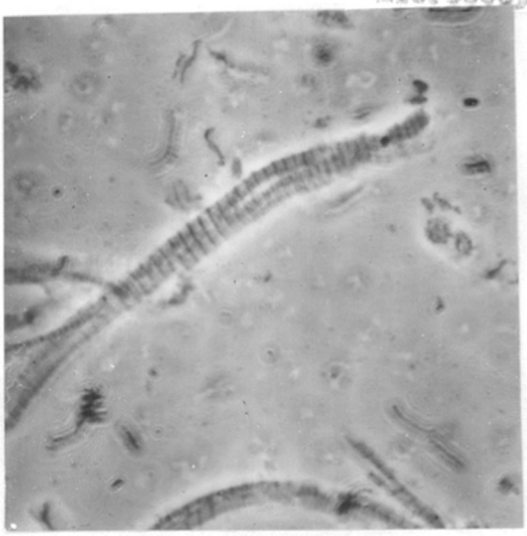

Fig. 50. Myofibrils from fresh rat diaphragm in 10% saline. By phase contrast illumination. 1200 x.

distribution of the myofibrils. As a further safeguard against fortuitous variations between different individuals, diaphragms in a similar state of activity were always taken from two or more animals.

Diaphragms were examined in the relaxed state, and the effect of stretching the muscle before fixing was studied; other diaphragms were stimulated electrically through the phrenic nerve, both isotonically, i.e. at constant tension, and isometrically, i.e. at constant length. The state of activity and the conditions during stimulation and fixation are listed below.

1. Relaxed muscle.
   (i) Fixed at rest length, i.e. without stretching.
   (ii) Fixed after passive stretching to live length.

2. Stimulated muscle.
   (i) Isotonically contracted muscle, stimulated at rest length, and fixed while contracted.
   (ii) Isotonically contracted muscle, stimulated at rest length but fixed after allowing to extend.
   (iii) Isometrically contracted muscle, stimulated at live length, and fixed while contracted.

Notes: The term rest length is used for the post mortem radial length of the muscular part of the diaphragm, and is about 12 mm. in the adult rat.

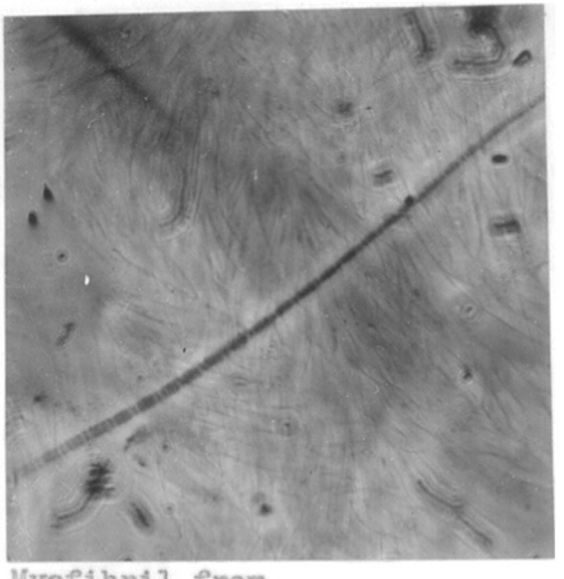

Fig. 51. Myofibril from rat diaphragm fixed in 10% formalin, by phase contrast illumination. 1200 x.

Fig. 52. Myofibrils from rat diaphragm, fixed in 10% formalin and dried, by phase contrast illumination. 500 x.

The term live length is used for the radial length of the muscular part of the diaphragm, and is estimated to be about 18 mm. in the live adult rat.

Stimulation was carried out in pulses of 2 m.secs. duration, and at the rate of 9 pulses/min.

(iii) Results.

Comparison of Fresh, Fixed and Dried Material by Phase Contrast Microscopy - Rat diaphragm muscle in saline solution, after fixing with 10% formalin, and after fixing and drying, was examined by phase contrast microscopy. The fresh muscle shows clear striations (Fig.50), but differentiation into the A, I and Z bands can only be distinguished in some parts of the field. On fixing, the three bands are found to stand out clearly (Fig.51), and drying does not affect the structure of the myofibril (Fig.52).

Pieces of sarcolemmal and connective tissues were observed in all samples.

The Types of Tissue Observed in the Electron Microscope - The electron beam was unable to penetrate through much of this material, but large numbers of striated "ribbons" were observed. Their widths varied between 0.5 - 1.0 μ, but the wider ribbons were often composed of several strands lying

side by side.

The narrowest components of these ribbons are the myofibrils mentioned in the introduction. In addition to sarcolemmal tissue and collagenous fibrils, similar to that reported by earlier workers (Hall, Jakus and Schmitt, 1946; Jones and Barer, 1948; Draper and Hodge, 1949), elastic fibrils from connective tissue could be identified in the electron microscope (Fig.53). The width of these fibrils was 0.1 μ in the dried and fixed material.

The Lengths of the A and I bands in Different States of Activity - A comparison of the lengths of the A and I bands of individual myofibrils in different states of activity can only be made in the electron microscope by comparing the length distribution in a number of myofibrils obtained from different diaphragms. The histograms (Fig.54) were obtained by measuring the A and I bands of myofibrils from relaxed diaphragm on the photographic plate, and relying on the magnification calibration of the instrument to obtain absolute values. The lowest set of histograms represents myofibrils from a number of relaxed diaphragms fixed at rest length, and the two other sets were each obtained from one rat. Both the extreme and the mean values in each set are slightly different from one another (Table IV), but it is evident that the limits containing 80% or more of the fibrils, and chosen as far as

Fig. 53. Electron micrograph of shadowed connective tissue fibrils from rat diaphragm, showing mainly elastic and some collagenous fibrils. Negative print. 5000 x.

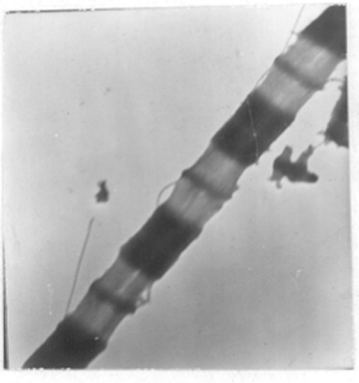

Fig. 56. Electron micrograph of myofibrils from rat diaphragm, showing acto-myosin filaments running along the length of the fibrils. 5000 x.

Table IV.

The Lengths of A and I Bands in Different Diaphragms.

No. of diaphragms.	No. of fibrils measured.	A		I	
		Limits of Length	Average Length.	Limits of Length	Average Length
		μ	μ	μ	μ
6	29	1.4-2.0	1.53	0.6-0.8	0.64
1	9	1.4-2.0	1.68	0.6-0.8	0.61
1	12	1.6-1.8	1.64	0.6-0.8	0.64

possible symmetrically about the mean value, show that no appreciable shift has occurred from one individual to the next. It is therefore permissible to compare the lengths of A and I in myofibrils from one diaphragm with those from another, provided that enough myofibrils are measured in each case, and that the limits (chosen as explained above), and not the mean values, are taken as standards of comparison.

Myofibrils from diaphragms in various states of activity were measured, and the measurements collected in the second set of histograms (Fig.55) and in Table V; the significance of the changes in length due to stretching, or stimulation, or both, will be discussed later.

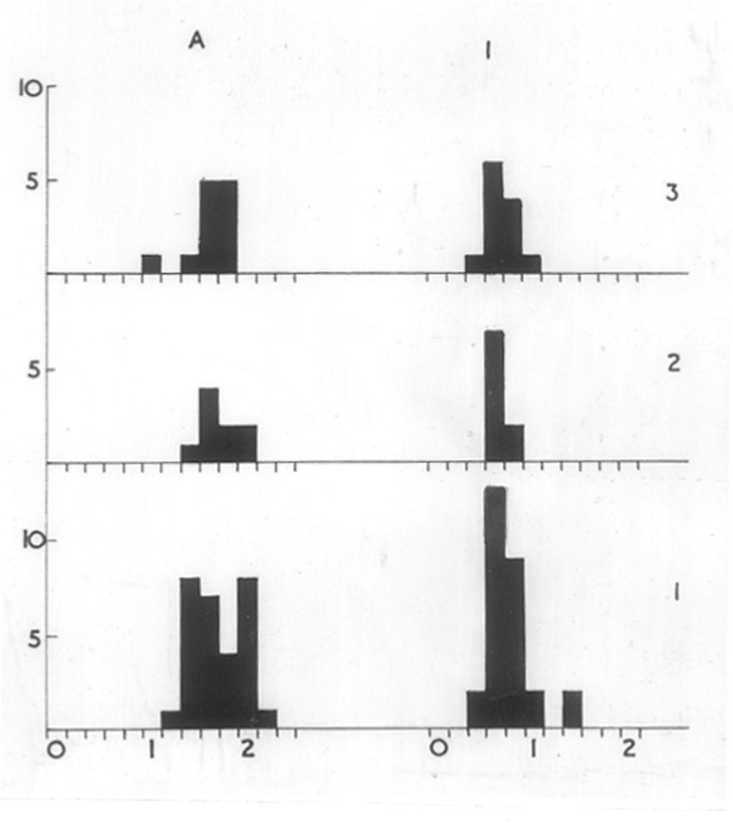

Fig. 54. Histograms giving the lengths in μ of the A and I bands of 50 myofibrils taken from different relaxed rat diaphragms.

Table V.

Changes in myofibril length in various physiological states.

I	II	III	IV
Physiological state of the diaphragm.	A.Bands Limits of length and average length. (in μ)	I.Bands Limits of length and average length. (in μ)	Sarcomeres Limits of length and average length. (in μ).
1. Relaxed, fixed at rest length.	1.4 - 2.0 (1.6)	0.6 - 0.8 (0.7)	2.0 - 2.8 (2.3)
2. Passively stretched to live length and fixed (compared with 1)	1.4 - 2.0 (1.6) Almost unchanged.	0.6 - 1.8 (1.0) Lengthened	2.0 - 3.4 (2.7) Lengthened
3. Isotonic contraction stimulated at rest length and fixed after allowing to lengthen. (compared with 1)	1.2 - 1.8 (1.5) Shortened.	0.6 - 1.4 (1.1) Lengthened	2.0 - 3.2 (2.6) Lengthened
4. Isotonic contraction stimulated at rest length and fixed while contracted. (compared with 1)	1.0 - 1.4 (1.2) Shortened	0.6 - 1.0 (0.7) Almost unchanged.	1.6 - 2.4 (1.9) Shortened
5. Isometric contraction stimulated at live length, and fixed while contracted. (compared with 2)	1.4 - 2.0 (1.7) Almost Unchanged	0.8 - 2.0 (1.2) Lengthened	2.2 - 3.8 (3.0) Lengthened

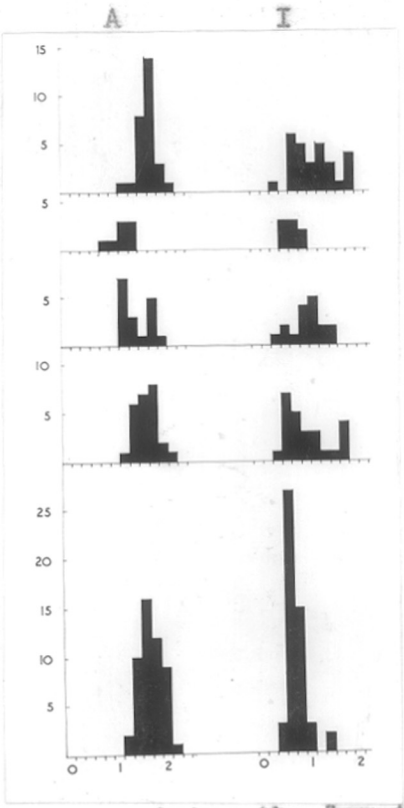

Fig. 55. Histograms giving the lengths (in μ) of the A and I bands of myofibrils taken from rat diaphragms in different states of activity. Starting from the bottom of the diagram:-

1. Relaxed and fixed at rest length.
2. Passively stretched to live length and fixed.
3. Isotonic contraction, stimulated at rest length and fixed after allowing to lengthen.
4. Isotonic contraction, stimulated at rest length, and fixed while contracted.
5. Isometric contraction, stimulated at live length and fixed.

The Incidence of H, M, and N. - Micrographs were obtained from myofibrils in addition to those shown in the histograms. In all but one of the physiological states listed above, H, M and N were very rarely encountered; the important exception was isometrically contracted material, stimulated at live length, where H, M, and N were found in most of the fibrils.

(iv) Discussion.

The Structure of the Myofibril - Muscle fibres were first seen to be striated by polarised light, which led to the present names of the A (anisotropic) and I (isotropic) bands (Bowman, 1840). It has since been found that the I band is also anisotropic, but to a smaller extent (Schmidt, 1935). The phase contrast microscope shows that, in addition, the A and I bands cause a different phase shift in light transmitted through them. There must, therefore, be some difference in the chemical composition, the crystalline structure, and/or the quantity of material present in the A and I bands. Within the limits imposed by the resolving power of the phase contrast microscope, a comparison of the optical and electron micrographs shows that those parts of the myofibril which cause a large phase shift (A, Z, and M) are the same parts which exhibit high electron scattering power. Electron micrographs of fixed and dried material further show that the

myosin or actomyosin filaments extend through both bands (Hall et al., 1946), although they are often obscured in the A band by the greater amount of solid matter found in the A band in addition to the actomyosin filaments (Fig.56).

It is now possible to describe the structure of the myofibril in greater detail. Its basic constituent is a fibrous protein, almost certainly myosin or actomyosin, held together by other less differentiated substances, certainly in the A, and possibly in the I band; at regular intervals, they are even more closely held together by the extra-fibrillar Z band, which also links them to neighbouring myofibrils.

The H Disc - The H disc is intra-fibrillar and must be regarded as a clear space resulting from a migration of the A substance towards its periphery. It is often associated with contraction, especially when stimulation is carried out at some degree of stretch. This has been observed before. Passive stretching alone, however, even when carried out after stimulation, does not produce the H disc.

The M Line - The M line is generally regarded as a membrane similar to the Z disc, but of a more delicate nature (Draper and Hodge, 1949). We are unable to accept this view at present, since the M line was not observed regularly in our materials except after stimulation at some degree of stretch.

Even in myofibrils which exhibited the H disc, the M line was not always present. In addition, no preferential fracture of the myofibrils at the M line was observed. While it is still possible that the M line may be extra-fibrillar, it seems unlikely. From the evidence available at present, it seems more likely to be an accumulation at the centre of the H disc of A substance left behind in its outward migration.

The N Lines - The N lines can often be resolved into a series of spots. The conditions under which they appear cannot be regarded as finally settled, and have been discussed elsewhere (Bluhm and Sitaramayya, 1951). They must be regarded as an unstable, intra-fibrillar structure.

Passive Stretching - Myofibrils from diaphragms passively stretched to their live length, show a definite increase in the length of the I bands, while the A bands show little or no change. This is in agreement with Hall's results for frog and rabbit leg muscles and with Landin's (1944) results for the frog cardiac muscle, but in contradiction to the results of Buchthal's school on similar fresh striated muscle.

It is improbable that fixation and consequent shrinkage could affect the results, for the effects of fixation on all the materials compared are similar and of small magnitude (10% shrinkage for fixation with 10% formalin, Høncke, 1947). It is possible, however, that diaphragm may behave differently

from other striated muscle, just as cardiac muscle is known to differ in its response to stretching, but this would still not explain the conflict of evidence for frog and rabbit muscle which has so far escaped attention, since Hall, Jakus and Schmitt believed their results to be in agreement with those of Buchthal's school.

Isotonic Contraction - Myofibrils from isotonically contracted diaphragm fixed in the contracted state show an overall shortening of the sarcomere, which is reflected in both the A and I bands. This is in agreement with the findings of the workers on similar material.

Isometric Contraction - The myofibrils from diaphragm in isometric contraction shown in Table V have longer sarcomeres than those of diaphragms stretched to live length. This indicates that the myofibrils were stretched to a greater length during stimulation. The I bands have lengthened, both as a result of stretching and of stimulation, but the A bands have remained practically unchanged, which is presumably due to the compensating effect of stretching and stimulation under these conditions.

Some Final Considerations - The relative constancy of the length of the A band in passive stretching, and its shortening during contraction indicate its essential role in the function of muscle. The greater extensibility of the I

band results in its overall lengthening during contraction under many conditions, so that its role in the contractile process would appear to be a comparatively minor one.

The myofibril is the smallest unit of striated muscle in which the contractile process has been observed in some detail. It would be of interest to extend these observations to the actomyosin filaments. This requires an increase in the effective resolution which might be brought about by increasing the accelerating voltage of the electron beam, and by inserting an objective aperture. This might, in turn, necessitate a more elaborate specimen preparation technique, such as freeze-drying, in order to preserve any finer structure which might be present.

3. THE STRUCTURE OF SILVER FILMS ON ROCKSALT CLEAVAGE FACES.

(i) Introduction.

Andrade and Martindale (1935) studied silver films deposited on quartz glass substrates by optical microscopy. They found that for films deposited at room temperature, the crystal size was less than 10^{-5} cm., and on heating the films to 230°C. or more, small aggregates and windows were formed. On heating to 600°C., they observed perfect cubic crystals, sometimes arranged along lines believed to be Griffith cracks. These authors observed discolouration of silver films deposited on rocksalt cleavage faces and therefore did not investigate them further.

A considerable amount of work has been done by electron diffraction on the structure of silver films grown epitaxially on the alkali halides. Silver films deposited on rocksalt cleavage faces at temperatures below 150°C. were largely random. Above 150°C., parallel growth was observed, and as the thickness of the film increased, the crystals were found to form lamellae by twinning on their {111} planes. Goche and Wilman (1939) heated the silver films for a few minutes in vacuo at temperatures between 500-600°C. after separating them from the substrate, and found that the

twinning had disappeared.

Hass (1942) investigated rapidly grown (2 - 60 secs.) silver films on rocksalt cleavage faces and obtained partially orientated deposits showing less graininess than those obtained on inert substrates. Johnson (1950) examined silver films on rocksalt cleavage faces by vertical illumination, using ordinary and polarised light. The agglomeration of the films was considered to be due to surface tension forces, and windows with straight edges orientated parallel to the ⟨110⟩ directions of the substrate were observed on heating the thicker films.

(ii) Interpretation.

Electron Micrographs - The measurements of crystal size were made by measuring the size of the smallest discrete entities on the photographic plate, and dividing this figure by the magnification of the instrument.

Electron Diffraction Patterns - The electron diffraction pattern is conveniently to be regarded as a section, enlarged by a factor of λL (where λ is the wavelength associated with the moving electrons and L the distance between the crystal and the photographic plate), through the origin of the reciprocal lattice of the crystal made by a plane parallel to the photographic plate. Silver (lattice constant a = 4.08 A)

forms a face centred cubic lattice, the corresponding reciprocal lattice being body centred cubic (lattice constant $a^* = 2/a$). Consequently, the diffraction pattern obtained with the beam along the cube edge of silver consists of a square network of spots, the sides of the square being $a^* \lambda L$, and parallel and perpendicular to the shadow edge. When the beam is along the cube face diagonals the diffraction pattern consists of a centred rectangular network of spots (side ratio $1:\sqrt{2}$), the smaller side being $a^* \lambda L$ and perpendicular to the shadow edge.

If the spots are drawn out towards the shadow edge along a certain reciprocal lattice row direction, the crystal face normal to that direction (and hence normal to the photographic plate) is well developed. The larger the number of scattering centres, the smaller the width of the diffraction beam, and hence the smaller is the size of the corresponding reciprocal lattice points; the converse is also true.

When silver is deposited on rocksalt some extra spots are usually observed in addition to the square and rectangular spot patterns. These spots fall into two categories:-

(a) Spots lying 1/6 of the way along the diagonal of the centred $\sqrt{2}$ rectangles; these are due to twinning on the

{111} planes of the original crystal, since the reciprocal lattice points of the {111} twins lie 1/6 of the way along the diagonals of the body centred cubic reciprocal lattice.

(b) The so-called irrational spots, which arise from the splitting up of each reciprocal lattice point into 4 component points on receding from the Bragg reflection position. These spots can be explained in terms of lamellar growth parallel to the {111} faces (usually due to repeated twinning on the {111} faces) as in this case the reciprocal lattice points are extended along <111> lattice rows normal to these planes (Stacheln or Spur theory, due to Laue, 1937).

If the crystals are randomly distributed, the diffraction pattern consists of rings. The radii of the rings correspond to the distances of the reciprocal lattice points from the origin.

The crystal size can be estimated from the width of the rings on a pattern due to randomly distributed crystals. For small crystals their diameter t in a direction at right angles to the beam is given by

$$t \approx 0.9 \frac{R.d}{\Delta R} ,$$

where d is the lattice spacing giving rise to the ring in question, R is its radius, and ΔR its half-width, i.e. the distance between the two points of the ring along the radius

at which its intensity has dropped to half its maximum value at the centre of the ring. This formula is approximate, since the value of the numerical constant depends on the shape of the crystal, and it breaks down for large crystals, giving rise to sharp rings when the width of the electron beam must be taken into account.

(iii) Experimental.

The silver films were obtained by slow evaporation (20-30 mins.) from an electrically heated silver wire supported at a distance of about 1.5 cms. from a freshly cleaved rocksalt cube face, in a vacuum of 10^{-2} - 10^{-3} mm. of Hg. The temperature of the vacuum chamber was controlled by heating its jacket with a Bunsen burner and the temperature of the chamber was measured with a thermocouple. A reflection pattern of the film was obtained in a Finch type electron diffraction camera (camera length 47 cms.). The film was then backed by a thin formvar film (p.53), and stripped by dissolving the crystal in water. Films which were heated after removal from the substrate were not backed with a formvar film. Part of the film was then picked up on an electron microscope grid, and part of it on a nickel gauze to obtain a transmission pattern in the electron diffraction camera. For both purposes the film was freeze-dried by placing it into a vacuum chamber, which was subsequently

evacuated, since this procedure seemed to give mechanically stronger films.

(iv) Results.

The results are set out in Table VI.

Table VI.

No.of film.	Description and Treatment of the film.	Features of Micrograph.	Description of the Diffraction Pattern.
1.	Deposited at 20°C. Dark blue by transmitted light.	A thin film showing small crystals (about 0.06 μ) and markings parallel to the cube edge of rocksalt.	The transmission pattern shows orientated {111} twinned lamellar crystals, and some randomly distributed crystals (crystal size 0.03 μ) (Fig.57). The reflection pattern shows mostly randomly distributed crystals, indicating that only the first few layers are epitaxial.
	Heated for 5 mins. to 500°C. after removing from substrate.	The micrograph remains unchanged, except that the crystal size has been increased to about 0.13 μ.	The structure of the film is now single crystal and shows some evidence of lamellar growth.
2.	Deposited at 20°C. Blue by transmitted light.	No micrograph was obtained since it was intended to heat the film on the substrate.	A reflection pattern shows mainly randomly distributed crystals, with some cube face orientation in the surface layers . (Fig.58).

	Heated on the substrate for 5 mins. to 570°C.	The micrograph shows rounded agglomerations which are sometimes arranged in lines (Fig.59).	The diffraction pattern shows lamellar growth and some randomly distributed crystals as well as an impurity.
3.	Deposited at 250°C. Dark grey by transmitted light.	Three types of film were observed in the electron microscope:-	
		(i) Structure not resolved.	Lamellar growth, and the film was bent.
		(ii) A continuous film with occasional structure.	The diffraction pattern is that of a single crystal.
		(iii) A thick film with irregular elongated gaps (Fig.60).	Large randomly distributed crystals, as well as parallel growth were observed.
	Heated to 600°C. for 5 mins. after removing from the substrate.	The micrograph shows a structure -less film with elongated gaps arranged to form parallel lines. The gaps are mainly in 4 directions at 45° to one another and parallel to the cube face diagonal of rocksalt (Fig.61).	The diffraction pattern is that of a single crystal, together with some contamination, identified from the pattern as Ag_2S.

4.	Deposited at 250°C. light blue, by transmitted light.	The film shows some holes and a fine structure indicating a crystal size of about 0.02 μ. (Fig.62).	Transmission patterns show parallel and lamellar growth. Some randomly distributed crystals, (crystal size 0.01 μ) and some impurity. A reflection pattern indicates a smooth surface, pronounced lamellar growth and twinning (Fig.63).
	Heated to 600°C. for 5 mins. after removing from substrate.	The film coagulated and broke up.	No diffraction patterns were obtained.
5.	Deposited at 530°C. yellow by transmitted light.	The film consisted of small crystals (~0.02 μ) and showed markings parallel to the cube edge. (Fig.64).	The reflection pattern shows parallel growth and some twinning; this is borne out by the transmission patterns, which in addition show some randomly distributed crystals (crystal size about 0,03 μ).

(v) Discussion.

The estimates of crystal size made from the electron micrographs and from the diffraction patterns gave results of the same order of magnitude, and it must be remembered that both methods are rough estimates only. The largest crystal size was found in a film deposited at room temperature, and this was further increased by subsequent heating after removing the film from the substrate.

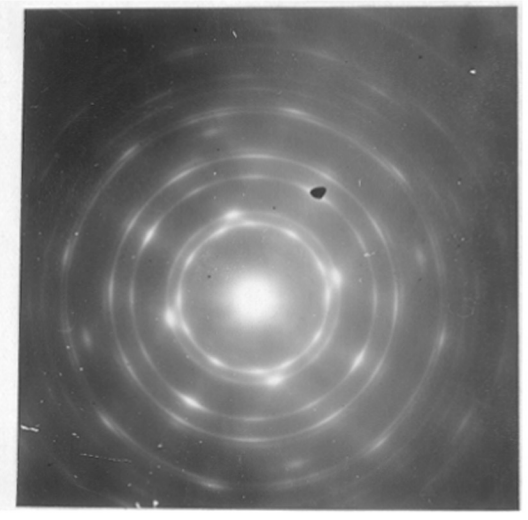

Fig. 57. Transmission electron diffraction pattern of silver film deposited on a rocksalt cleavage face at room temperature.

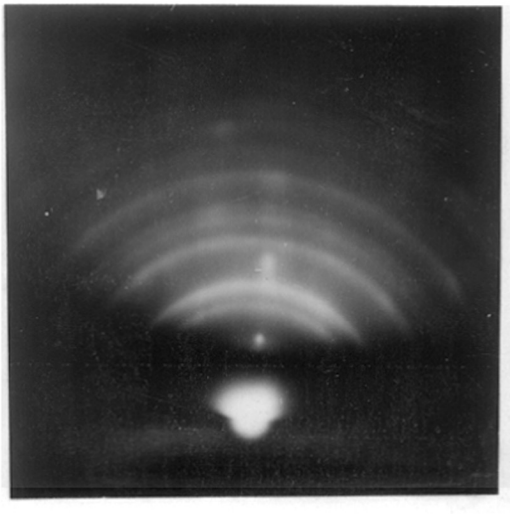

Fig. 58. Reflection electron diffraction pattern of a silver film deposited on a rocksalt cleavage face at room temperature.

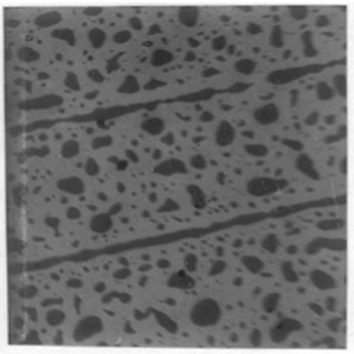

Fig. 59. Electron micrograph of a silver film deposited on a rocksalt cleavage face at room temperature, and heated on the substrate to 570°C. 5000 x.

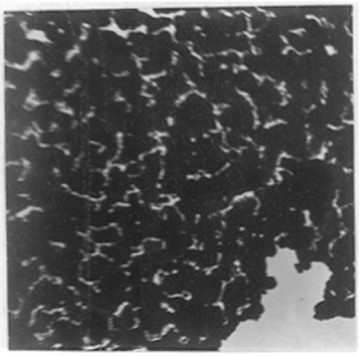

Fig. 60. Electron micrograph of a silver film deposited on a rocksalt cleavage face at 250°C., 5000 x.

Fig. 61. The same film as fig. 60, but heated to 600°C after removing it from the substrate. 2000 x.

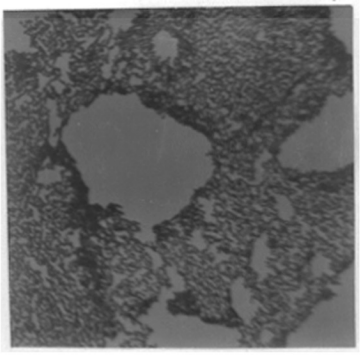

Fig. 62. Electron micrograph of a silver film deposited on a rocksalt cleavage face at 250°C. 10,000 x.

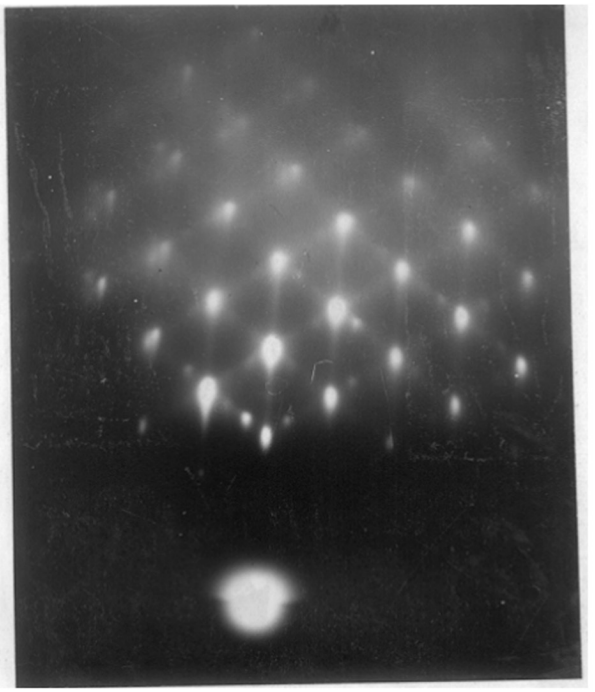

Fig. 63. Reflection electron diffraction pattern of the silver film shown in fig. 62.

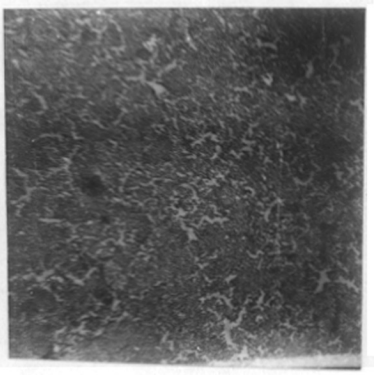

Fig. 64. Electron micrograph of a silver film deposited on a rocksalt cleavage face at 530°C. 5000 x.

The most striking observation made in the course of this work is the wide variety of external shapes containing a narrow range of atomic arrangements. No correlation was found between the appearance of the micrograph and the structure as revealed by the diffraction pattern.

The cleavage steps on the substrate were reproduced by some of the silver films while in others they only exerted some influence on the arrangement of agglomerations and holes in the film.

The film heated on the substrate shows rounded aggregates which may be regarded as the consequence of surface tension as suggested by Johnson (1950). Heating after removing the film from the substrate results in the formation of holes or in the breaking up of the film.

It is felt that the resolving power of the present electron microscope was not adequate for revealing detail on a scale which could be correlated with the information afforded by the electron diffraction patterns.

4. CONCLUSIONS.

The resolving power of the optical microscope is limited to about 2400 A. by the wavelength of light, and no further improvement can be expected in this respect. Phase contrast microscopy for transmitted and incident light has been developed recently, and has provided sufficient contrast in specimens which could hitherto not be examined successfully except after appropriate treatment, such as etching or staining. In addition, for many different types of specimen, the appearance and significance of the phase contrast image is similar to that of the electron micrograph, and consequently a phase contrast microscope is a valuable aid to the electron microscopist.

The electron microscope in its present form has an optimum resolving power of about 10 A., and Gabor (1949) has made certain proposals which may lead to a resolving power of 1 A. This limitation is not imposed by the wavelength associated with the moving electron, but rather by our inability to construct wide aperture electron lenses which are free from aberration. Only specimens up to about 1 μ in thickness (or replicas of surfaces not showing greater variations in height) can be examined by electron microscopy, and in addition the structure of the specimen must remain significant after drying, inserting into a high vacuum and

heating as a result of the bombardment by the electron beam.

In the course of the present work these conditions have been fulfilled by a variety of methods. The Beilby layer formed on glass as a result of polishing was studied by a simple replica method, which was rendered more informative by shadowing. The shape and particle size of the polishing powders could be observed directly after spreading a random sample on a supporting film. The structure (on an electron microscopic scale) of mammalian muscle fibres could be stabilised sufficiently by formalin fixation and subsequent staining to permit direct examination by electron microscopy. It is, however, inherent in both these methods of specimen preparation that significant electron diffraction patterns cannot be obtained.

The crystal structure of silver films grown on rocksalt cleavage faces had previously been studied by electron diffraction, and the shape and size of the particles in a few of these films were therefore observed in the electron microscope.

Perhaps the most promising result of this work was the evidence given by the electron microscope of the formation of rounded aggregates (Fig.59) as a result of heating the film on the substrate. Electron diffraction showed that these aggregates were still crystalline. This instance shows that the electron microscope is capable of giving useful information

about crystalline films, provided that the size of the crystals is such that they can be resolved.

Acknowledgements.

I should like to thank Professor G.I.Finch, F.R.S. for his interest and his encouragement by numerous helpful suggestions and discussions throughout the course of my work.

It was a pleasure to be associated with Mr. C. Sitaramayya during the work on diaphragm muscle fibrils, and I should like to thank Dr.C.F.Challice for his kind permission to reproduce Fig.5.

Finally, thanks are due to the Ministry of Education for a maintenance grant made under the Further Education and Training Scheme from 1947-49.

REFERENCES.

The references, indicated in the text by the name of the author(s) and the year of publication, are grouped in six sections, the order being alphabetical within each section.

1. Optical Microscopy.

Abbe, 1873, Archiv.f.Mikr.Anat., 9, 413.

Airy, 1835, Camb.Phil.Trans., 5, 283.

Brice, 1947, F.I.A.T. Final Report No.1059 and Suppl.No.1 H.M.Stationery Office.

Burch and Stock, 1942, J.Sci.Inst., 19, 71.

Conrady, 1904, J.Roy.Micr.Soc., 163, 610.

Conrady, 1905, J.Roy.Micr.Soc., 168, 541.

Cooke, Troughton and Simms Ltd., Photomicrography with the Vickers Projection Microscope.

Cuckow, 1949, J.Iron and Steel Inst., 161, 1.

Helmholtz., 1874, Pogg.Ann. Jubel band.

Johnson, 1928, J.Roy.Micr.Soc., 48, 144.

Kohler and Loos, 1941, Naturw., 29, 49.

Lummer and Reiche, 1910, Die Lehre von der Bildentstehung im Mikroskop, von E.Abbe. Brunswick.

Martin, 1931, Proc.Phys.Soc., 43, 186.

Martin, 1932, An Introduction to Applied Optics, Chap. III.

Martin and Johnson, 1949, p.72 Practical Microscopy, London.

Oettle, 1950, J.Roy.Micr.Soc., 70, 232.

Osterberg, 1946, J.Opt.Soc.Amer., 36, 469.

Paine, 1950, J.Roy.Micr.Soc., 70, 225.

Rayleigh, 1896, Phil.Mag., 42, 167.

Taylor, 1947, Proc.Roy.Soc., A.190, 422.

Zernike, 1935, Z.tech.Phys., 16, 454.

Zernike, 1942, Physica, 9, 648 and 974.

2. Electron Microscopy.

v.Ardenne, 1938, Z.Phys., 108, 338.

v.Borries, 1949, Die Uebermikroskopie, Saenger, Berlin.

Brown, 1949, Ph.D.Thesis, London.

Busch, 1926, Ann.d.Phys., 81, 974.

Challice, 1949, Ph.D.Thesis, London.

Cosslett, 1946, Proc.Phys.Soc., 58, 443.

Cosslett (Ed.), 1950, Bibliography of Electron Microscopy, Arnold, London.

Davisson and Germer, 1927, Nature, 119, 558.

Dawson, 1950, J.Sci.Inst., 27, 142.

v.Dorsten, Oosterkamp and Le Poole, Philips Tech.Rev., 9, 193.

Drummond (Ed.), 1950, The Practice of Electron Microscopy, J.Roy.Micr.Soc., 70, March issue.

Gabor, 1942-3, Electr.Eng., 295, 328, 372, 15.

Gabor, 1947, The Electron Microscope, Hulton Press, London.

Gabor, 1949, Proc. Roy. Soc. A, 197, 454. 1949.

Haine, Page and Garfitt, 1950, J.Appl.Phys., 21, 173.

Hesse, 1948, Ph.D.Thesis, London.

Hillier, 1940, Phys.Rev., 58, 842.

Hillier, 1948, J.Appl.Phys., 19, 121.

Hillier, 1949, J.Bact., 57, 313.

Hillier and Ramberg, 1947, J.Appl.Phys., 18, 48.

Hillier and Vance, 1941, Proc.Inst.Radio Engrs., 29, 167.

Knoll and Ruska, 1932, Z.Phys., 78, 318.

Le Poole, 1947, Philips Tech.Rev., 9, 33.

Lewis, 1950, Ph.D.Thesis, London.

Scherzer, 1936, Z.Phys., 101, 593.

Thomson and Reid, 1927, Nature, 119, 890.

Wyckoff, 1949, Electron Microscopy, Interscience Publishers, New York and London.

Zworykin, Morton, Ramberg, Hillier and Vance, 1945, Electron Optics and the Electron Microscope, Wiley, N.Y.

3. The Electron Diffraction Camera.

Finch and Quarrell, 1933, Proc.Roy.Soc., A.141, 399.

Thomson and Fraser, 1930, Proc.Roy.Soc., A.128, 641.

4. The Scratching and Polishing of Glass Surfaces.

Beilby, 1921, The Aggregation and Flow of Solids, Macmillan, London.

Bowden and Ridler, 1936, Proc.Roy.Soc., A.154, 640.

Brown, 1949, Ph.D.Thesis, London.

Custers, 1949, Nature, 164, 627.

Deacon, Ellis, Cross and Sennett, 1948, J.Appl.Phys., 19, 704.

Finch, Quarrell and Roebuck, 1934, Proc.Roy.Soc., A.145, 676.

Finch, Quarrell and Wilman, 1935, Trans.Far.Soc., 31, 1051.

Finch, 1937, Trans.Far.Soc., 33, 425.

Finch and Whitmore, 1938, Trans.Far.Soc., 34, 640.

Golz, 1943, Z.Phys., 120, 773.

Griffith, 1921, Phil.Trans. A.221, 163.

Kamogawa, 1940, Phys.Rev., 58, 660.

Leise, 1948, Z.Phys., 124, 258.

Marx, Klemm and Smekal, 1941, Naturw., 29, 668.

Maxwell and Mosley, 1935, Phys.Rev., 47, 331.

Newton, 1704, Opticks.

Raether, 1948, Z.Phys., 124, 286.

Rayleigh, 1901, Proc.Roy.Inst., 16, 563.

Royer, 1928, Bull.Soc.franc.Mineral., 51, 7.

5. The Structure of Striated Muscle.

Barer, 1948, Biol.Rev., 23, 159.

Beams, Evans, Jenny and Baker, 1949, Anat.Rec., 105, 59.

Bluhm and Sitaramayya, 1951, In course of publication.

Bowman, 1840, Philos.Trans., 130, 457.

Buchthal, Knappeis and Lindhard, 1936, Skand.Arch.Physiol., 73, 162.

Draper and Hodge, 1949, Aust.J.exp.Biol., 27, 465.

Draper and Hodge, 1950, Aust.J.exp.Biol., 28, 549.

Hall, Jakus and Schmitt, 1945, J.Appl.Phys., 16, 459.

Hall, Jakus and Schmitt, 1946, Biol.Bull., 90, 32.

Høncke, 1947, Acta Physiol.Scand., 15, Suppl.48.

Lundin, 1944, Acta Physiol.Scand., 7, Suppl.20.

Pease and Baker, 1949, Amer.J.Anat., 84, 175.

Richards, Anderson and Hance, 1942, Proc. Soc.exp.Biol. N.Y., 51, 148.

Schmidt, 1935, Z.Zellf., 23, 201.

Szent-Györgyi, 1946, J.Coll.Sci., 1, 1.

6. The Structure of Silver Films.

Andrade and Martindale, 1935, Phil.Trans.Roy.Soc., 235, 69.

Goche and Wilman, 1939, Proc.Phys.Soc., 51, 625.

Hass, 1942, Kolloid Z., 100, 230.

Johnson, 1950, J.Appl.Phys., 21, 449.

Laue, 1937, Ann.Phys. Lpz., 29, 211.